Theses and Dissertations

12-2017

An Evaluation of Borehole Hydraulic Conductivity Equations and Field Determined Soil Water Characteristic Curves

Johnathan Dale Blanchard
University of Arkansas, Fayetteville

www.manaraa.com

An Evaluation of Borehole Hydraulic Conductivity Equations and Field Determined Soil Water
Characteristic Curves

A thesis submitted in partial fulfillment
of the requirements for the degree of
Master of Science in Civil Engineering

by

Johnathan Blanchard
University of Arkansas
Bachelor of Science in Civil Engineering, 2015

December 2017
University of Arkansas

This thesis is approved for recommendation to the Graduate Council.

_____

Dr. Richard Coffman
Thesis Director

_____

Dr. Michelle Bernhardt-Barry
Committee Member

_____

Dr. Findlay Edwards
Committee Member

ABSTRACT

The methods utilized to determine the hydraulic conductivity of compacted clay liners (CCLs) are of importance for safe guarding the environment from landfill leachate. Therefore, the methods utilized in the analysis of the Two Stage Borehole (TSB) test, as described in the ASTM D6391-11 (Method A, B, and C) standard, were evaluated. Data from hydraulic conductivity tests, as performed on three test pads, were utilized to review the ASTM D6391-11 equations. Additionally, two test pads were instrumented with volumetric water content and soil water matric potential sensors to facilitate the determination of field-obtained soil water characteristic curves (SWCCs) and hydraulic conductivity functions (k-functions) for unsaturated soils. For the determination of the SWCCs and k-functions, each test pad was subjected to an infiltration cycle, using either a sealed double ring infiltrometer or a two-stage borehole infiltrometer, followed by a drying cycle. To compare the results that were obtained from the field-obtained SWCCs and k-functions, laboratory tests were performed on Shelby tube samples acquired from the corresponding test pad. The obtained data were fitted using the van Genuchten model and the RETC (RETention Curve) program.

The results that were obtained from TSB testing led to the conclusion that Method B and C, as written in the ASTMs D6391-11 standard contained errors that impacted the results that were obtained from hydraulic conductivity testing. Specifically, utilizing Method C provided results that were four times greater than the hydraulic conductivity and utilizing Method B provided results that were as much as two orders of magnitude greater than the hydraulic conductivity. Several recommendations are proposed herein to ensure accurate hydraulic conductivity analysis is performed in the future. It was further determined that a poor agreement

exists between field-obtained and laboratory-obtained k-functions and SWCCs, as reported in

other studies. Therefore, field-obtained k-functions are preferential, when available.

DEDICATION

This thesis is dedicated to all of the people who made it possible. To my family who were always encouraging, my parents: Clifford and Julie Blanchard, my siblings: Miranda, Cassandra, and Samuel, my girlfriend: Kristen Burger and my late mother: Klaashia Blanchard – who installed in me an early interest in the sciences. I also acknowledge the great faculty at the University of Arkansas, chief and foremost, my advisor Dr. Richard Coffman. I was rarely a great student, but you were always a great advisor, mentor, and role model. I appreciate those few individuals who challenged me to do more, even if I did not heed their advice, in no particular order: Natalie Becknell, Dr. Michelle Bernhardt-Barry, Phil Carroll, Dr. Findlay Edwards, and Dr. Ernie Heymsfield. Finally, thank you to my friends and colleagues who helped me along the way, in no particular order: Cyrus Garner, Elvis Ishimwe, Nabeel Mahmood, Connor Malpass, Sean Salazar, Anh Tran, Matthew Voss, and everyone at the Rock House.

TABLE OF CONTENTS

LIST OF FIGURES

LIST OF TABLES

LIST OF PUBLISHED OR SUBMITTED PAPERS

Chapter 3: Review of the Equations Used to Calculate Hydraulic Conductivity Values from Two-Stage Borehole Tests. Submitted as: *Blanchard, J.D., Nanak, M., Coffman, R.A., (2017). "A Review of the Two-Stage Borehole Method." Journal of Testing and Evaluation. Manuscript Number: JTE-2017-0028.R3. Submitted for Review on November 20th, 2017.*

Chapter 4: Field-Obtained Soil Water Characteristic Curves and Hydraulic Conductivity Functions. Published as: *Ishimwe, E., Blanchard, J.D., and Coffman, R.A., "Field-Obtained Soil Water Characteristic Curves and Hydraulic Conductivity Functions," Journal of Irrigation and Drainage Engineering, Vol. 144, No. 1. DOI: 10.1061/(ASCE)IR.1943-4774.0001272.*

CHAPTER 1: INTRODUCTION

1.1. Chapter Overview

Two investigations relating to the testing and performance of compacted clay liners, typical of landfill liner applications, are described in this document. Specifically, the various testing methods utilized for two-stage borehole testing, which is commonly used to test and validate landfill liners, were evaluated for the first investigation. Whereas, the soil water characteristic curves and hydraulic conductivity functions, obtained from laboratory methods were compared with field-obtained curves during the second investigation. The field-obtained and laboratory-curves were compared to determine if the laboratory-obtained curves were representative. Within this chapter: A brief overview of the two investigations is presented in Section 1.2, The motivations for the two investigations are presented in Section 1.3, and an overview for the entire document is provided in Section 1.4.

1.2. Description of Work

The construction and hydraulic conductivity testing of field-scale Compacted Clay Liners (CCLs) using laboratory-scale test pads are described in this document. The testing was performed as part of an investigation into the methods utilized to evaluate the hydraulic conductivity of CCLs. Five test pads were utilized to evaluate two different testing techniques. Specifically, the Two-Stage Borehole (TSB) testing methods, as described in ASTM D6391 (2011), were evaluated with Test Pad1, Test Pad 2, and Test Pad 5. The Sealed Double Ring Infiltrometer (SDRI) testing method, as described in ASTM 5093 (2015), was evaluated using Test Pad 3 and Test Pad 4. Additionally, in-situ instrumentation were installed and utilized in Test Pads 4 and Test Pad 5 to investigate the Soil Water Characteristic Curves (SWCCs), as obtained in situ rather than as obtained in the laboratory, which is the current industry standard.

1

The work conducted by the author was associated with Test Pad 5, which was utilized to 1) evaluate the TSB methods and to 2) obtain in situ SWCCs. The steps of the field-obtained SWCC, which included the TSB testing in Test Pad 5, are displayed in Figure 1.1. The development of the Test Pad testing program is detailed in Maldonado and Coffman (2012) and Nanak (2012).

Field-Scale Testing

Compacted Clay Liner (CCL)

Laboratory-Scale (Validation) Testing

Sealed Double Ring Infiltrometer (SDRI)

In-situ Instruments

Two-Stage Borehole (TSB)

Soil Sampling after Drying Cycle

K_{field}

$SWCC_{field}$

K_{field}

$SWCC_{field}$

Shelby Tube Specimens

WP4

TRIM

Flexible Wall Permeability

$SWCC_{lab}$

K_{lab}
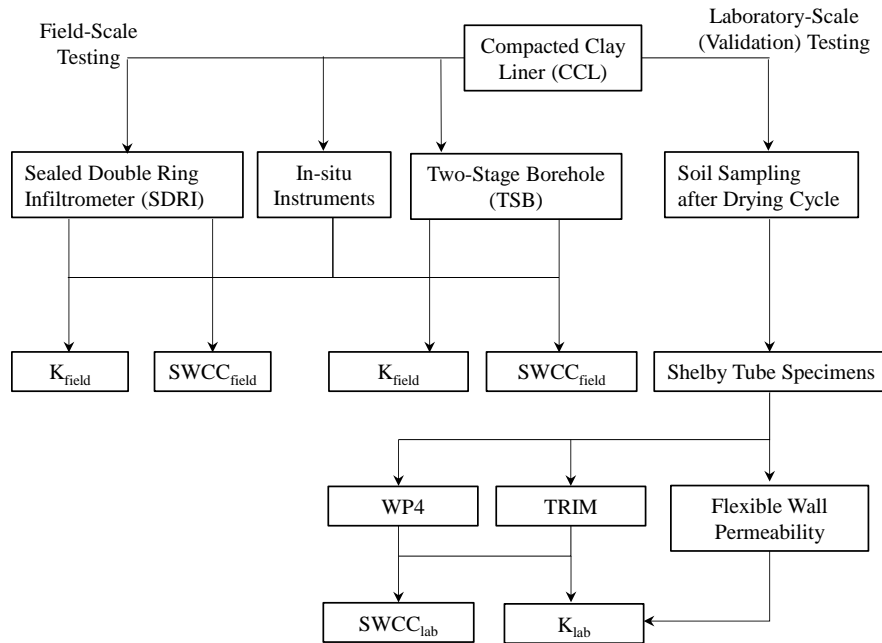
Figure 1.1. Flowchart of the testing program (modified from Ishimwe et al. 2017).

1.3. Motivation

The implementation of regulations (i.e. Arkansas Regulation Number 22 and EPA Subtitle D) has successfully improved landfill operations and helped to reduce the impact of landfill facilities on the environment; however, the regulations rely upon the methods that are utilized to evaluate and enforce the regulatory requirements. Due to the stringent nature of regulatory requirements, and due to the difficulty of obtaining operating permits, the need for accurate and expedient testing results is of paramount importance. Consequently, in-situ tests, like the two-stage borehole test and the sealed double ring infiltrometer test, have been utilized to meet this need.

2

The two-stage borehole test was developed in 1983 by Dr. Gordon Boutwell to measure the in-situ hydraulic conductivity of soils (STEI, 1983). Since the inception of the TSB test, several data reducing methods have been codified (Figure 1.2), but no comprehensive evaluation of these methods has been disseminated. Due to the vital function that these tests serve in ensuring the hydraulic conductivity for landfill liners are within regulatory limits, an evaluation of the different methods was necessary. The literature review and the testing program that were conducted, and described in this document, fulfilled the needed evaluation.
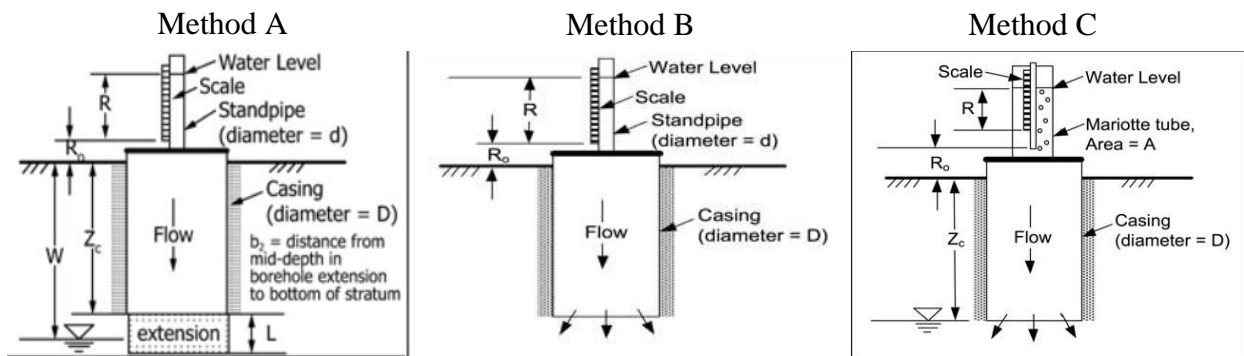
Figure 1.2. Different methods for calculating hydraulic conductivity according to ASTM D6391 (2011).

TSB tests, as well as other in-situ tests, are used to determine the saturated hydraulic conductivity. The saturated hydraulic conductivity is the greatest expected value of hydraulic conductivity and may not be appropriate for all applications. As reported in Fredlund and Rahardjo (1993), many of the geotechnical engineering problems (e.g., slope stability, shallow and deep foundations failures following rainfall, swelling and shrinkage of clays) that occur in arid and semiarid climatic areas are associated with unsaturated soils. Therefore, a better understanding of the unsaturated soils behavior is necessary for designing various geotechnical structures.

3

The time and cost of the soil testing that is required to determine unsaturated soil properties have been reduced by utilizing SWCCs and k-functions. Like with other soil phenomena (strength, permeability, compressibility), these characteristic functions have historically been measured in the laboratory (Wang and Benson, 2004; Mijares and Khire, 2010; Wyllace and Lu, 2012; ASTM D6836, 2008) with the results then being applied to determine the full-scale field responses. Although SWCCs have frequently been obtained in the laboratory, some field measurements of SWCCs have been completed using field-testing equipment (Watson et al., 1975; Tzimas, 1979; Li et al., 2004). Therefore, further comparison between SWCCs obtained from laboratory testing equipment and SWCCs obtained from in situ field testing equipment is necessary to ensure that laboratory-obtained results are representative of field conditions. The comparison, as derived from the testing program described in this document, is reported. Moreover, recommendations regarding usage of SWCCs are also reported.

1.4. Document Overview

An introduction and overview of the work conducted are provided in this chapter (Chapter 1). A literature review is provided in Chapter 2. Manuscripts that have been submitted for journal publication are presented in Chapters 3 and 4, with the manuscripts being presented in the chronological order in which the work associated with each manuscript was performed. Specifically, an evaluation of different TSB testing methods is presented in Chapter 3 and details about the development of field-obtained SWCCs and k-functions are presented in Chapter 4. Conclusions drawn from the results presented in Chapters 3 and 4 are presented in Chapter 5. A comprehensive list of references used in this document is included in Chapter 6.

4

1.5. References

ASTM (2015). "Standard test methods for field measurement of infiltration using double-ring infiltrometer with sealed-inner ring." Annual Book of ASTM Standards, Designation D 5093-15, Vol. 4.08, ASTM, West Conshohocken, PA.

ASTM (2011), "Standard test method for field measurement of hydraulic conductivity using borehole infiltration" Annual Book of ASTM Standards, Designation D 6391-11, Vol. 4.08, ASTM, West Conshohocken, PA.

ASTM (2016), "Standard test methods for determination of the soil water characteristic curve for desorption using a hanging column, pressure extractor, chilled mirror hygrometer, and/or centrifuge." Annual Book of ASTM Standards, Designation D6836-16, West Conshohocken, PA.

Fredlund, D. G. and Rahardjo, H. (1996). Soil mechanics for unsaturated soils, John Wiley and Sons Inc., New York.

Li, A. G., Tham, L. G., Yue Z. Q., Lee, C. L., and Law K. T. (2004). "Comparison of field and laboratory soil-water characteristic curves." J. Geotech. Geoenviron. Eng., 10.1061/ (ASCE) 1090-0241(2005)131:9(1176), 1176-1180.

Maldonado, C., and Coffman, R. (2012). "Hydraulic conductivity of environmentally controlled landfill liner test pad." ASCE Geotechnical Special Publication No. 225, Proc. GeoCongress 2012: State of the Art and Practice in Geotechnical Engineering, Oakland, California, 3593-3602.

Mijares, R.G. and Khire, M.V. (2010). "Soil water characteristic curves of compacted clay subjected to multiple wetting and drying cycles." GeoFlorida 2010: Advances in Analysis, Modeling and Design, ASCE, 400-409.

Nanak, M. J. (2012). "Variability in the hydraulic conductivity of a test pad liner system using different testing techniques." Master's Thesis, University of Arkansas.

Soil Testing Engineers, Inc. (1983). "STEI two-stage field permeability test." Soil Testing Engineers, Inc., Baton Rouge, LA.

Tzimas, E. (1979). "The measurement of soil water hysteretic relationship on a soil monolith." J. Soil Sci., Vol. 30, 529-534.

Wang, X. and Benson, C. (2004). "Leak-free pressure plate extractor for measuring the soil water characteristic curve." Geotechnical Testing Journal, Vol. 27, No. 2, pp.1-10.

Wayllace, A., and Lu, N. (2012). "A transient water release and imbibitions method for rapidly measuring wetting and drying soil water retention and hydraulic conductivity functions." Geotechnical Testing Journal, Vol. 35, No. 1, 1-15.

Watson, K.K., Reginato, R. J., and Jackson, R. D. (1975). "Soil water hysteresis in a field soil." Soil Sci. Soc. Am. Proc., Vol. 39, 242-246.

CHAPTER 2: BACKGROUND

2.1. Chapter Overview

A review of relevant literature is contained in this chapter. The in-situ methods for determining hydraulic conductivity are presented in Section 2.2. A discussion on different methods utilized to determine soil water characteristic curves is presented in Section 2.3.

2.2. In-situ Hydraulic Conductivity

There are two industry accepted approaches for determining hydraulic conductivity from a TSB test, 1) the time lag approach which was originally proposed by Hvorslev (1951) using well equations and 2) the velocity method that was proposed by Chapuis (1999). Several other authors have also contributed complementary literature regarding the way in which these two methods have been applied.

Soil Testing Engineers, Inc. (STEI, 1983) presented the TSB test in 1983 using Case "C" and Case "G" equations from Hvorslev (1951) to calculate K1 and K2, respectively. For Stage 1 of the TSB test, a borehole is augered into the soil to the depth of interest, and an open bottom casing (typically polyvinylchloride [PVC]) is then grouted into place with bentonite. The casing prevents lateral flow as the permeant enters the soil. The apparent vertical hydraulic conductivity is obtained by monitoring the quantity of permeant entering the soil as a function of time. For Stage 2, soil is removed from the bottom of the borehole by augering to a specified depth below the depth of the bottom of the casing. The increased depth permits the permeant to flow in the lateral direction, through the uncased section of the newly formed borehole. The apparent horizontal conductivity within the soil is determined during this stage. The hydraulic conductivity values determined during Stage 1 (K1) and Stage 2 (K2) correspond to the maximum expected value of the vertical hydraulic conductivity (k_v) and the minimum expected value of the horizontal hydraulic conductivity (k_h), respectively.

6

The STEI (1983) method also utilized an anisotropy factor, identified as "m", to resolve the apparent values of hydraulic conductivity (K1 and K2) into vertical and horizontal hydraulic conductivity (k_v and k_h) values. The value of "m" was originally selected from a table utilizing the length to diameter ratio of the extended borehole and the ratio of K1 to K2, but can now be directly determined by using an equation solver. The Soil Testing Engineers, Inc. (1983), method was presented by Daniel (1989) with some minor changes in terminology. The method presented by Daniel (1989) included a chart, rather than a table, to estimate the value of "m". Boutwell (1992) presented new time lag equations, which although still based on the Hvorslev (1951) equations, included a temperature viscosity correction term and additional geometric constants (G) to account for differing boundary conditions. Boutwell (1992) also introduced a new method to estimate "m", as based upon the geometric constants. Boutwell and Tsai (1992) presented corrections for several typographical errors found within Boutwell (1992) and simplified the terminology utilized for calculating the geometric constants. Additional corrections were provided in Trautwein and Boutwell (1994).

The first version of the ASTM D6391 standard, about the TSB method, was presented in 1999 (ASTM D6391, 1999). The method presented in Boutwell (1992), Boutwell and Tsai (1992), and Trautwein and Boutwell (1994) were presented in the standard to calculate the apparent hydraulic conductivity values (methods to determine "m" were not included). In 2006, the ASTM D6391 (2006) standard was released; the ASTM D6391 (2006) differed from the ASTM D6391 (1999) standard because metric units were used as the primary units within the standard. Two additional methods for calculating apparent hydraulic conductivity are included in the most current version of the ASTM D6391 standard (ASTM D6391, 2011). These newly included methods consist of a velocity head method (Method B) and a constant head method

7

(Method C). The constant head test method was derived directly from Hvorslev (1951). The velocity method was derived in Chapuis (1999) and is discussed in more detail later in this document. The original ASTM D6391 (1999) method, based on the Boutwell (1992) method, was referred to as Method A in the ASTM D6391 (2011) standard. The equations for Method A are presented in Equations 2.1 through 2.9. Additionally, the STEI (1983) method for determining anisotropy from Method A is presented in Equation 2.10 and 2.11 and the equation utilized in Method C is presented in Equation 2.12.

$$K1 = \frac{R_t G_1 \ln\left(\frac{Z_1}{Z_2}\right)}{(t_2 - t_1)}$$
(ASTM D6391, 2011)   [2.1]

$$K2 = \frac{R_t G_2 \ln\left(\frac{Z_1}{Z_2}\right)}{(t_2 - t_1)}$$
(ASTM D6391, 2011)   [2.2]

$$R_t = \frac{2.2902\left(0.9842^T\right)}{T^{0.1702}}$$
(ASTM D6391, 2011)   [2.3]

$$G1 = \left(\frac{\pi d^2}{11D}\right)\left[1 + a\left(\frac{D}{4b_1}\right)\right]$$
(ASTM D6391, 2011)   [2.4]

$$G2 = \left(\frac{d^2}{16FL}\right)G3$$
(ASTM D6391, 2011)   [2.5]

$$G3 = 2\ln(G4) + a\ln(G5)$$
(ASTM D6391, 2011)   [2.6]

$$G4 = \frac{L}{D} + \left[1 + \left(\frac{L}{D}\right)^2\right]^{1/2}$$
(ASTM D6391, 2011)   [2.7]

$$G5 = \frac{\left[\frac{4b_2}{D} + \frac{L}{D}\right] + \left[1 + \left(\frac{4b_2}{D} + \frac{L}{D}\right)^2\right]^{1/2}}{\left[\frac{4b_2}{D} - \frac{L}{D}\right] + \left[1 + \left(\frac{4b_2}{D} - \frac{L}{D}\right)^2\right]^{1/2}}$$
(ASTM D6391, 2011)   [2.8]

$$F = 1 - (0.5623)e^{-1.566\left(\frac{L}{D}\right)}$$
(ASTM D6391, 2011)   [2.9]

8

$$\frac{K2'}{K1'} = m\frac{\ln\left[\dfrac{L}{D}\sqrt{1+\left(\dfrac{L}{D}\right)^2}\right]}{\ln\left[\dfrac{mL}{D}+\sqrt{1+\left(\dfrac{mL}{D}\right)^2}\right]}$$ (ASTM D6391, 2011) [2.10]

$$K1' = k_v m = \frac{k_h}{m}$$ (ASTM D6391, 2011) [2.11]

$$k = \frac{\pi\left(d_s^2 - d_m^2\right)\left(z_1 - z_2\right)}{2.75D\left(k_b\right)\left(t_2 - t_1\right)}$$ (ASTM D6391, 2011) [2.12]

In Equations 2.1 through 2.12, d is the internal diameter (ID) of the standpipe; $D1$ is the ID of the casing; b_1 is the thickness of the tested soil below the casing; Z_1 is the effective head at the beginning of the time increment; Z_2 is the effective head at the end of the time increment; t_1 is the time at the beginning of the increment(s); t_2 is the time at the end of the increment(s); R_T is the temperature correction factor used to convert k to k_{20} (k at 20°C); T is temperature (in Celsius); b_2 is equal to ($b_1 - L/2$); L is the length of the Stage 2 extension; a is 1 if the base at b_1 is impermeable, a is 0 for an infinite thickness, and a is -1 if the base at b_1 is permeable; $K1'$ is the time weighted average for the temporally invariant period for K1; $K2'$ is the time weighted average during the temporally invariant period for K2; m is determined by using the Excel solver function from Equation 2.10; d_s is equal to the ID of the standpipe; d_m is equal to the outer diameter (OD) of the Mariotte tube; and k_b is the total head acting on the soil ($k_b = H$).

Chapuis (1999) did not agree with the time lag approach for determining hydraulic conductivity, stating that time lag methods assume: 1) that an impermeable top layer was used, 2) that an inaccurate ellipsoid flow shape was suggested, and 3) that the anisotropy factor could not be solved. Additionally, Chapuis (1999) believed that the boundary conditions utilized in the time lag methods were not representative of field conditions (assuming the location of the piezometric line). Chapuis (1999) stated that these assumptions enabled practitioners to manipulate testing results. In contrast to the time lag approach, Chapuis (1999) proposed a velocity-based method for calculating hydraulic conductivity. A velocity graph was suggested by Chapuis (1999) to determine the hydraulic conductivity value. The location of the piezometric

9

line is determined using the velocity graph. This method latter adapted by Chiasson (2005) to account for perceived scatter in the data at lower values of hydraulic conductivity. The ASTM D6391-11 Method B (2011) is similar to the method proposed by Chiasson (2005). The equations for Method B are presented as Equations 2.13 through 2.16.

$$Z_t = Z^* + Z_0 \exp(-at) \qquad \text{(ASTM D6391, 2011)} \qquad [2.13]$$

$$min\left(\frac{1}{n}\sum_{i=1}^{n}(Z_i - Z_{ti})^2\right) \qquad \text{(ASTM D6391, 2011)} \qquad [2.14]$$

$$\sum_{i=1}^{n}(Z_i - Z_{ti}) = 0 \qquad \text{(ASTM D6391, 2011)} \qquad [2.15]$$

$$k = R_t a \frac{\pi d^2}{11D} \qquad \text{(ASTM D6391, 2011)} \qquad [2.16]$$

In Equations 2.13 through 2.16, Z_i is the height from the ground surface to the water in the standpipe at time i; Z_{ti} is the fitted value of Z at time i; H^* is a fitting parameter related to total head; H_0 is a fitting parameter related to initial head; and a is a fitting parameter related to the hydraulic conductivity. Equation 2.14 is minimized and is constrained by Equation 2.15.

In practice, the methods proposed in ASTM D6391 (2011) are utilized when performing a TSB test. Consequently, the methods in ASTM D6391 (2011) were the primary focus of this study; however, it is important to note that the methods in the ASTM D6391 (2011) standard were derived from the earlier methods and earlier standards (i.e. the 1999 and 2006 ASTM D 6391 Standards). Evaluations of these methods, and standards, were performed by Nanak (2012) and Blanchard (2015) to evaluate the accuracy and efficiency of each method proposed in the ASTM D6391 (2011) standard.

Another in-situ method that has been utilized is the sealed double ring infiltrometer. The equations [Equation 2.17 and 2.18] proposed by Daniel and Trautwein (1986) are commonly used for calculating the in-situ hydraulic conductivity value from SDRI test data. Three methods,

previously presented in Trautwein and Boutwell (1994), are commonly utilized to determine the hydraulic gradient (i), as required to calculate hydraulic conductivity (k). These three methods include 1) the wetting front method (Equation 2.19), 2) the suction head method (Equation 2.20), and 3) the apparent hydraulic conductivity method (Equation 2.21). SDRI and TSB testing methods have been shown to give comparable results as reported in Nanak (2012).

$$k = \frac{I}{i} F \qquad \text{(Daniel Trautwein, 1986)} \qquad [2.17]$$

$$I = \frac{Q}{tA} \qquad \text{(Daniel Trautwein, 1986)} \qquad [2.18]$$

$$i = \frac{H + Z_w}{Z_w} \qquad \text{(Nanak, 2012)} \qquad [2.19]$$

$$i = \frac{H + Z_w + H_s}{Z_w} \qquad \text{(Nanak, 2012)} \qquad [2.20]$$

$$i = \frac{H + Z}{Z} \qquad \text{(Nanak, 2012)} \qquad [2.21]$$

Within Equations 2.17 through 2.21, I is the infiltration rate, Q is the volume of flow, t is the sub-test time duration, A is the area of infiltration, F is the correction factor to account for lateral spreading of water, H is the head of water above the soil surface, H_s is the suction head at the location of the wetting front, Z_w is the depth of wetting front below the soil surface, and Z is the depth of the test pad.

2.3. Methods of Determining Soil Water Characteristic Curves

According to Lu et al. (2014), the hydraulic conductivity of soil should not be considered a constant value. Instead, the hydraulic conductivity of soil is a function of the degree of saturation and the amount of suction (matric potential) within the soil (Ishimwe, 2014). Soil Water Characteristic Curves (SWCCs) and Hydraulic Conductivity Functions (k-functions) have been used to represent unsaturated soil properties for many years (Klute et al. 1986, Fredlund et al. 1994, Fredlund 1995, Fredlund and Rahardjo 1996, Fredlund et al. 1996, Fredlund and Xing 1997, Lu and Likos 2004, Lu and Kaya 2013). Utilizing tools, like the SWCC and k-functions to

account for unsaturated hydraulic properties are required for efficient design of clay liners, as well as other applications.

As documented within the literature, several laboratory techniques exist for measuring the SWCC (Klute et al. 1986; Wang and Benson 2004; Mijares and Khire 2010; Wayllace and Lu 2012; ASTM D 6836 2016). Two specific methods utilized to determine SWCCs in a laboratory setting include the transient water release and imbibitions methods (TRIM) and the chilled mirror hygrometer method (WP4).

The WP4 test was reported to be one of the most accurate ways to determine laboratory SWCCs by Samingan and Schanz (2005). The WP4 method correlates dew point to soil suction by measuring the relative humidity within a closed system. Humidity measurements that involve chilling a reflective surface to a temperature at which condensation occurs and then measuring the intensity at which a transmitted light is reflected from the mirror, are correlated to the soil suction in Lu and Likos (2004). The WP4 test was originally utilized for soil suction by Gee et al. (1992).

The TRIM method was originally developed by Wayllace and Lu (2012). The TRIM device, necessary for TRIM testing, applies a transient flow to a given soil specimen under different levels of pressure. The water content is then determined through inverse modeling. Although the technique is relatively new, it has been shown to produce comparable results to other laboratory techniques. Also, continuous rather than discrete data are produced from the TRIM method.

It has been reported in the literature that SWCCs are sensitive to factors such as molding water content, compactive effort, and stress state (Malaya and Sreedeep 2012, Tinjum et al. 1997). Laboratory-obtained SWCCs are often determined utilizing disturbed or completely

12

disturbed samples (Garner, 2017), which can affect sensitive SWCC factors and alter the resulting curve. Because laboratory-obtained curves are applied to field conditions, laboratory-obtained curves must be validated for in situ field conditions.

Although laboratory testing techniques are numerous, few field-scale methods have been developed to determine SWCCs (Watson et al. 1975; Tzimas 1979; Li et al. 2004; Ogorzalek et al. 2008). Specifically, Watson et al. (1975) measured the field SWCC using 1) triangular pyramid frame housing instrumentation to determine water content and 2) tensiometers to measure the soil water pressure. Li et al. (2004) measured the field-scale SWCCs at the crest and berm of a large cut slope in Hong Kong using the time domain reflectometry probes and vibrating wire tensiometers to measure water content and soil suction, respectively. Likewise, Ogorzalek et al (2008) used time domain reflectometry probes and thermal dissipation sensors to define the SWCC for a capillary barrier cover in Polston, Montana (Ishimwe, 2014).

2.4. References

ASTM (2016), "Standard test methods for determination of the soil water characteristic curve for desorption using a hanging column, pressure extractor, chilled mirror hygrometer, and/or centrifuge." *ASTM D6836-16*, West Conshohocken, PA.

ASTM (1999), "Standard test method for field measurement of hydraulic conductivity limits of porous materials using two stages of infiltration from a borehole" Annual Book of ASTM Standards, Designation D 6391-99, Vol. 4.08, ASTM, West Conshohocken, PA.

ASTM (2006), "Standard test method for field measurement of hydraulic conductivity limits of porous materials using two stages of infiltration from a borehole" Annual Book of ASTM Standards, Designation D 6391-06, Vol. 4.08, ASTM, West Conshohocken, PA.

ASTM (2015), "Standard test method for field measurement of hydraulic conductivity using borehole infiltration" Annual Book of ASTM Standards, Designation D 6391-11, Vol. 4.08, ASTM, West Conshohocken, PA.

Blanchard, J, (2015). Evaluation of the equations used to calculate hydraulic conductivity values from two-stage borehole tests, *Honors Thesis*, University of Arkansas, May 2015

Boutwell, G., (1992). "The STEI two-stage borehole field permeability test." Containment Liner Technology and Subtitle D, Houston Section, ASCE, Houston, TX.

Boutwell, G. and Tsai, C., (1992). "The two-stage field permeability test for clay liners." *Geotechnical News*, C. Shackelford and D. Daniel, eds., pp. 32-34.

Chapuis, R., (1999). "Borehole variable-head permeability tests in compacted clay liners and covers." *Canadian Geotechnical Journal*, Vol. 36, pp. 39-51.

Chiasson, P., (2005). "Methods of interpretation of borehole falling-head tests performed in compacted clay liners." *Canadian Geotechnical Journal*, Vol. 42, pp. 79-90.

Daniel, D., (1989). "In situ hydraulic conductivity tests for compacted clay." *Journal of Geotechnical Engineering*., ASCE, Vol. 115, No. 9, pp. 1205-1226.

Fredlund, D. G., Xing, A., and Huang, S. (1994). "Predicting the permeability function for unsaturated soils using the soil-water characteristic curve." *Canadian Geotechnical Journal*, Ottawa, Canada, Vol. 31, No. 4, 1994, 533-546.

Fredlund, D.G. (1995). "Prediction of unsaturated soil functions using the soil-water characteristic curve." unsaturated soils group department of civil engineering. University of Saskatchewan, 57 Campus Drive, Canada, 1995.

Fredlund, D. G. and Rahardjo, H. (1996). Soil mechanics for unsaturated soils, *John Wiley and Sons Inc.*, New York.

Fredlund, M. D., Sillers, W. S., Fredlund, D. G. and Wilson, G. W. (1996). "Design of a knowledge-based system for unsaturated soil properties." *Proceedings of the Canadian Conference on Computing in Civil Engineering,* Montreal, Quebec, August 26-28, pp. 659-677.

Fredlund, D. and Xing, A. 1997. "Equations for the soil water characteristic curve." *Canadian Geotechnical Journal*, Vol. 3, No. 4, 533-546.

Garner, C. (2017). "Development of a multiband remote sensing system for determination of unsaturated soil properties." Doctoral Dissertation, University of Arkansas.

Gee, G., M. Campbell, G. Campbell, and J. Campbell. 1992. Rapid measurement of low soil potentials using a water activity meter. Soil Sci. Soc. Am. J. 56:1068–1070

Hvorslev, J., (1951). "Time lag and soil permeability in ground water observations." Bulletin No. 36, United States Army Corps of Engineers, Waterways Experiment Station, Vicksburg, MS.

Ishimwe, E, (2014). Field-obtained soil water characteristic curves and hydraulic conductivity functions. Masters Thesis, University of Arkansas, May 2013.

Klute, A. Campbell, G.S. Jackson, D. Mortiland, M.M. and Nielson, D.R. (1986). "Methods of soil analysis." Part 1, *Physical and Mineralogical Methods, Second Edition,* American Society of Agronomy and Soil Science of America, Madison, Wisconsin, 810 pgs.

Li, A. G., Tham, L. G., Yue Z. Q., Lee, C. L., and Law K. T. (2004). "Comparison of field and laboratory soil-water characteristic curves." *J. Geotech. Geoenviron. Eng.*, 10.1061/ (ASCE) 1090-0241(2005)131:9(1176), 1176-1180.

Lu, N. and Likos, W.J. (2004). Unsaturated soil mechanics, *John Wiley and Sons*, New Jersey, USA, 556 pgs.

Lu, N., and Kaya, M. (2013). "A drying cake method for measuring suction stress characteristic curve, soil-water retention, and hydraulic conductivity function." *Geotechnical Testing Journal,* Vol. 36, pp. 1–19.

Malaya, C., & Sreedeep, S. (2012). Critical review on the parameters influencing soil-water characteristic curve. *Journal of Irrigation and Drainage Engineering*, 138(1), 55-62.

Mijares, R.G. and Khire, M.V. (2010). "Soil water characteristic curves of compacted clay subjected to multiple wetting and drying cycles." *GeoFlorida 2010: Advances in Analysis*, *Modeling and Design,* ASCE, 400-409.

Nanak, M, (2013). Variability in the Hydraulic Conductivity of a Test Pad Liner System Using Different Testing Techniques. Masters Thesis, University of Arkansas, May 2013.

Ogorzalek A. S., Bohnholf G.L., Shackelford C. D., Benson, C. H., and Apiwantragoon. (2008). "Compaction of field data and water-balance predictions for a capillary barrier covers." *J. Geotech. Geoenviron. Eng.*, 10.1061/(ASCE)1090-0241(2008)134:4(470), 470-486.

Samingan, A., & Schanz, T. (2005). "Comparison of four methods for measuring total suction." *Vadose Zone Journal,* 4(4), 1087-1095.

Soil Testing Engineers, Inc. (1983). *STEI Two-Stage Field Permeability Test*. Soil Testing Engineers, Inc., Baton Rouge, LA.

Tinjum, J.M., Benson, C.H., and Boltz, L.R,.(1997). "Soil-water characteristic curves for compacted clays." *Journal of geotechnical and geoenvironmental engineering* 123, no. 11: 1060-1069.

Trautwein, S. and Boutwell, G. (1994). "In situ hydraulic conductivity tests for compacted soil liners and caps." *Hydraulic Conductivity and Waste Contaminant Transport in Soil*, STP 1142, D. Daniel and S. Trautwein, eds., ASTM, Philadelphia, pp. 184-223.

Tzimas, E. (1979). "The measurement of soil water hysteretic relationship on a soil monolith." *J. Soil Sci.,* Vol. 30, 529-534.

Wang, X. and Benson, C. (2004). "Leak-free pressure plate extractor for measuring the soil water characteristic curve." *Geotechnical Testing Journal*, Vol. 27, No. 2, pp.1-10.

Watson, K.K., Reginato, R. J., and Jackson, R. D. (1975). "Soil water hysteresis in a field soil." *Soil Sci. Soc. Am. Proc.,* Vol. 39, 242-246.

Wayllace, A., and Lu, N. (2012). "A transient water release and imbitions method for rapidly measuring wetting and drying soil water retention and hydraulic conductivity functions." *Geotechnical Testing Journal*, Vol. 35, No. 1, 1-15.

CHAPTER 3: REVIEW OF THE EQUATIONS USED TO CALCULATE HYDRAULIC CONDUCTIVITY VALUES FROM TWO-STAGE BOREHOLE TESTS

3.1. Chapter Overview

In this chapter, the methods utilized to conduct and interrupt two-stage borehole (TSB) test data are analyzed and reviewed. Specifically, the three methods, as presented, in the ASTM D6391-11 (Method A, B, and C) standard were considered. A literature review concerning the evolution of the different methods was conducted and an experimental testing program was performed. For this study three compacted clay liners were tested in a laboratory setting and the results from the different TSB testing methods were compared with each other and with the results from flexible wall permeability testing on the same soil. Several errors were observed in ASTM D6391-11 standard and are discussed.

The limitations of the submitted journal manuscript, that is presented in this chapter, are discussed in Section 3.2. The full citation for manuscript is included in Section 3.3. Moreover, the motivation for the manuscript that is contained in this chapter is discussed in Sections 3.4 and 3.5. The background of the TSB test and the research study detailed in the manuscript are detailed in Section 3.6. Descriptions of the methodologies and procedures for the testing program, test pad construction and testing, calibration of data sheets, and the comparison between Method A and Method B are presented in Section 3.7.1, 3.7.2, 3.7.3, and 3.7.4, respectively. The results from the research are presented in Section 3.8; specifically, from the results from TSB testing, calibration of data sheets, and the comparison between Method A and Method B are presented in Section 3.8.1, 3.8.2, and 3.8.3, respectively. Finally, conclusions and recommendations for the TSB testing methods are presented in Section 3.9.

3.2. Limitations of the Described Study

The manuscript contained in this chapter is limited to the TSB testing methodologies that were presented in ASTM D6391 (2011). Although ASTM D6391 (2011) represents the major methodologies utilized by practitioners, other data reduction methods exist for determining hydraulic conductivity from the TSB test. Many of the varying methods were discussed in the background section of the manuscript (Section 3.6), but the review is by no means exhaustive, nor are non-ASTM methods utilized in the comparison of TSB testing results. However, Nanak (2011) did consider many of the non-ASTM methods. However, the velocity method proposed by Chapuis (1999) (which corresponds to ASTM D6391 Method B) are not well represented by Nanak (2011); the velocity method was only discussed in relation to Method B in the manuscript in this chapter.

3.3. Review of the Equations Used to Calculate Hydraulic Conductivity Values from Two-Stage Borehole Tests

Reference
Blanchard, J.D., Nanak, M., Coffman, R.A., (2017). "A Review of the Two-Stage Borehole Method." Journal of Testing and Evaluation. Manuscript Number: JTE-2017-0028.R3. Submitted for Review on November 20th, 2017.

3.4. Abstract

The methods to determine the hydraulic conductivity of compacted clay liners utilizing two-stage borehole (TSB) tests were investigated. Specifically, the methods described in the ASTM D6391-11 (Method A, B, and C) standard, were evaluated. Data from hydraulic conductivity tests, as performed on three test pads, were utilized to review the ASTM equations. The obtained results led to the conclusion that Method B and C, as written in the ASTMs D6391-11 standard contained errors that significantly impacted the results of hydraulic conductivity

18

testing. Therefore, several recommendations are proposed herein to ensure accurate hydraulic conductivity analysis is performed in the future.

Keywords: Hydraulic Conductivity, In-situ field testing, Constant Head, Falling Head, Two-Stage Borehole.

3.5. Introduction

Since the mid-1970s there has been a growing emphasis on protecting the environment from exposure to municipal solid waste. This emphasis has led to new regulations about the way in which municipal waste is disposed of and stored. Many regulations (i.e. Arkansas Regulation Number 22 and EPA Subtitle D) require landfills to encapsulate municipal waste by using a compacted clay liner (CCL). Typically, a CCL is placed within an acceptable placement window (acceptable water content and corresponding acceptable dry density) that ensures the hydraulic conductivity value (k) for the soil is less than the regulated requirement of 1E-07 cm/s. The purpose of such regulations is to limit the amount of leachate that can infiltrate into the groundwater.

The implementation of regulations has successfully improved landfill operations and the impact of landfill facilities on the environment; however, the regulations rely upon the methods that are utilized to evaluate and enforce the regulatory requirements. Due to the stringent nature of regulatory requirements, and due to the difficulty of obtaining operating permits, the need for accurate and expedient testing results is paramount. Consequently, the two-stage borehole (TSB) test has been utilized to meet this need.

The two-stage borehole test was developed in 1983 by Dr. Gordon Boutwell (STEI, 1983) to measure the in-situ hydraulic conductivity of soils. Since the inception of the TSB test, several test methods were proposed (Figure 3.1), but no comprehensive evaluation of these

19

methods has been disseminated within the literature. The discussion found herein is a review of the evolution and the efficacy of different TSB test methods that have been reported within the literature. Additionally, the methods and results of a testing program conducted at the University of Arkansas (UofA), which evaluated the three testing methods reported within the ASTM D6391 (2011) standard, are reported and discussed. Finally, the results and conclusions drawn from this review and testing program are reported.
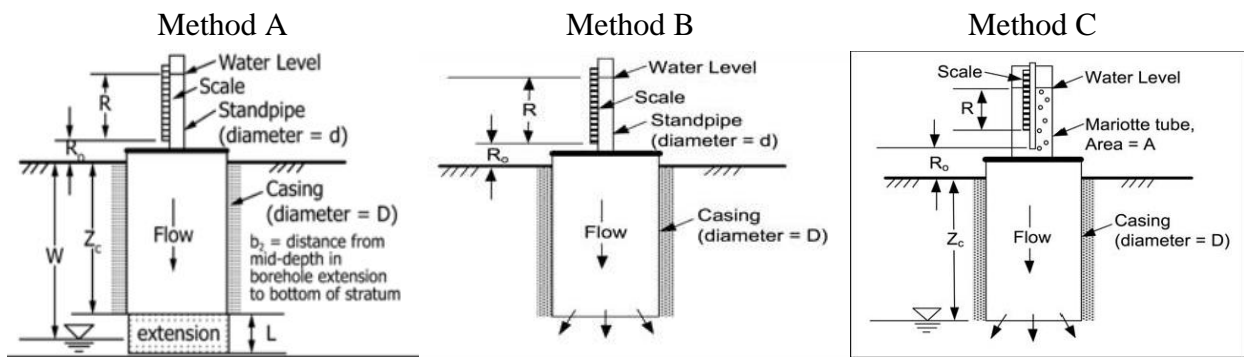
Figure 3.1. Different methods for calculating hydraulic conductivity according to ASTM D6391 (2011).

3.6. Background

There are two industry accepted approaches for determining hydraulic conductivity from a TSB test, 1) the time lag approach which was originally proposed by Hvorslev (1951) using well equations and 2) the velocity method that was proposed by Chapuis (1999). Several other authors have also contributed complimentary literature regarding the way in which these two methods have been applied.

Soil Testing Engineers, Inc. (STEI, 1983) presented the TSB test in 1983 using Case "C" and Case "G" equations from Hvorslev (1951) to calculate K1 and K2, respectively. For Stage 1 of the TSB test, a borehole is augered into the soil to the depth of interest, and an open bottom casing (typically polyvinylchloride [PVC]) is grouted into place. The casing prevents lateral flow

20

as the permeant enters the soil. By monitoring the volume of permeant entering the soil, it is possible to calculate the vertical hydraulic conductivity of the soil. For Stage 2, the soil is augered from the bottom of the borehole to a specified depth extending below the depth of the casing. This permits the permeant to flow in the lateral direction, through the uncased section of the borehole, and allows for the determination of the horizontal flow rate within the soil. The hydraulic conductivity values determined during Stage 1 (K1) and Stage 2 (K2) correspond to the maximum expected value of the vertical hydraulic conductivity (k_v) and the minimum expected value of the horizontal hydraulic conductivity (k_h), respectively.

The STEI (1983) method also utilized the anisotropy factor "m" to resolve the apparent values of hydraulic conductivity (K1 and K2) into vertical and horizontal hydraulic conductivity (k_v and k_h) values. The value of "m" was selected from a table utilizing the length to diameter ratio of the borehole and the ratio of K1 to K2, but can now be solved for directly using a solver tool. The Soil Testing Engineers, Inc., method was presented again by Daniel (1989) with some minor changes in terminology. The method presented by Daniel (1989) also included a chart, rather than a table, for estimating the value of "m". Boutwell (1992) presented new time lag equations, which although still based on Hvorslev (1951) equations, included a temperature viscosity correction term and additional geometric constants (G) to account for differing boundary conditions. Boutwell (1992) also introduced a new method for estimating "m", based upon the geometric constants. Boutwell and Tsai (1992) presented corrections for several typographical errors found within Boutwell (1992) and simplified the terminology utilized for calculating the geometric constants. Additional corrections were presented by Trautwein and Boutwell (1994).

21

In 1999 the first publication of the ASTM D6391 (1999) standard was presented. The standard utilized the method presented in Boutwell (1992), Boutwell and Tsai (1992), and Trautwein and Boutwell (1994) to calculate the apparent hydraulic conductivity values (methods to determine "m" were not included). In 2006, the ASTM D6391 (2006) standard was released, which updated the 1999 publication by making metric units the primary units within the standard. The 2011 version of ASTM D6391 (2011) is the current version and includes two additional methods for determining the apparent hydraulic conductivity. These methods consist of a velocity head method (Method B) and a constant head method (Method C). The constant head test method was derived directly from Hvorslev (1951) and the velocity method is discussed in more detail later. The original ASTM D6391 (1999) method, based on Boutwell (1992) was titled Method A. The equations for Method A and presented in Equations 3.1 through 3.9. Additionally, the STEI (1983) method for determining anisotropy from Method A is presented in Equation 3.10 and 3.11 and the equation utilized in Method C is presented in Equation 3.12.

$$K1 = \frac{R_t G_1 \ln\left(\frac{Z_1}{Z_2}\right)}{(t_2 - t_1)}$$
(ASTM D6391, 2011)   [3.1]

$$K2 = \frac{R_t G_2 \ln\left(\frac{Z_1}{Z_2}\right)}{(t_2 - t_1)}$$
(ASTM D6391, 2011)   [3.2]

$$R_t = \frac{2.2902\left(0.9842^T\right)}{T^{0.1702}}$$
(ASTM D6391, 2011)   [3.3]

$$G1 = \left(\frac{\pi d^2}{11D}\right)\left[1 + a\left(\frac{D}{4b_1}\right)\right]$$
(ASTM D6391, 2011)   [3.4]

$$G2 = \left(\frac{d^2}{16FL}\right)G3$$
(ASTM D6391, 2011)   [3.5]

22

$$G3 = 2\ln(G4) + a\ln(G5) \qquad \text{(ASTM D6391, 2011)} \qquad [3.6]$$

$$G4 = \frac{L}{D} + \left[1 + \left(\frac{L}{D}\right)^2\right]^{1/2} \qquad \text{(ASTM D6391, 2011)} \qquad [3.7]$$

$$G5 = \frac{\left[\dfrac{4b_2}{D} + \dfrac{L}{D}\right] + \left[1 + \left(\dfrac{4b_2}{D} + \dfrac{L}{D}\right)^2\right]^{1/2}}{\left[\dfrac{4b_2}{D} - \dfrac{L}{D}\right] + \left[1 + \left(\dfrac{4b_2}{D} - \dfrac{L}{D}\right)^2\right]^{1/2}} \qquad \text{(ASTM D6391, 2011)} \qquad [3.8]$$

$$F = 1 - (0.5623)e^{-1.566\left(\frac{L}{D}\right)} \qquad \text{(ASTM D6391, 2011)} \qquad [3.9]$$

$$\frac{K2'}{K1'} = m\frac{\ln\left[\dfrac{L}{D}\sqrt{1 + \left(\dfrac{L}{D}\right)^2}\right]}{\ln\left[\dfrac{mL}{D} + \sqrt{1 + \left(\dfrac{mL}{D}\right)^2}\right]} \qquad \text{(ASTM D6391, 2011)} \qquad [3.10]$$

$$K1' = k_v m = \frac{k_h}{m} \qquad \text{(ASTM D6391, 2011)} \qquad [3.11]$$

$$k = \frac{\pi\left(d_s^2 - d_m^2\right)\left(z_1 - z_2\right)}{2.75D\left(k_b\right)\left(t_2 - t_1\right)} \qquad \text{(ASTM D6391, 2011)} \qquad [3.12]$$

In Equations 3.1 through 3.12, d is the internal diameter (ID) of the standpipe; D1 is the ID of the casing; b_1 is the thickness of the tested soil below the casing; Z_1 is the effective head at the beginning of the time increment; Z_2 is the effective head at the end of the time increment; t_1 is the time at the beginning of the increment(s); t_2 is the time at the end of the increment(s); R_T is the temperature correction factor used to convert k to k_{20} (k at 20^0 C); T is temperature (in Celsius); b_2 is equal to ($b_1 - L/2$); L is the length of the Stage 2 extension; a is 1 if the base at b_1 is impermeable, a is 0 for an infinite thickness, and a is -1 if the base at b_1 is permeable; K1' is the time weighted average for the temporally invariant period for K1; K2' is the time weighted average during the temporally invariant period for K2; m is determined by using the Excel solver function and Equation 3.10; d_s is equal to the ID of the standpipe; d_m is equal to the outer diameter (OD) of the Mariotte tube; and k_b is the total head acting on the soil (k_b= H).

Chapuis (1999) did not agree with the time lag approach for determining hydraulic

conductivity, stating that time lag methods assume: 1) an impermeable top layer, 2) an inaccurate

23

ellipsoid flow shape, and 3) that the anisotropy factor could not be solved. Additionally, Chapuis (1999) believed that the boundary conditions utilized in the time lag methods were not representative of field conditions (assuming the location of the piezometric line), and enabled practitioners to manipulate results. In contrast to the time lag approach, Chapuis (1999) proposed a velocity based method for calculating hydraulic conductivity. The velocity method utilizes the velocity graph to determine hydraulic conductivity and corrects for the location of the piezometric line. This method was latter adapted by Chiasson (2005) to account for perceived scatter in the data at lower values of hydraulic conductivity. ASTM D6391 (2011) Method B is similar to the method proposed by Chiasson (2005). The equations for Method B are presented as Equations 3.13 through 3.16.

$$Z_t = Z^* + Z_0 \exp(-at) \qquad \text{(ASTM D6391, 2011)} \qquad [3.13]$$

$$min\left(\frac{1}{n}\sum_{i=1}^{n}(Z_i - Z_{ti})^2\right) \qquad \text{(ASTM D6391, 2011)} \qquad [3.14]$$

$$\sum_{i=1}^{n}(Z_i - Z_{ti}) = 0 \qquad \text{(ASTM D6391, 2011)} \qquad [3.15]$$

$$k = R_t a \frac{\pi d^2}{11D} \qquad \text{(ASTM D6391, 2011)} \qquad [3.16]$$

In Equations 3.13 through 3.16, Z_i is the height from the ground surface to the water in the standpipe at time i; Z_{ti} is the fitted value of Z at time i; H^* is a fitting parameter related to total head; H_0 is a fitting parameter related to initial head; and a is a fitting parameter related to the hydraulic conductivity. Equation 3.14 is minimized and is constrained by Equation 3.15.

In practice, the methods proposed in ASTM D6391 (2011) are typically utilized when performing a TSB test. Consequently, the methods in ASTM D6391 (2011) were the primary focus of this study; however, it is important to note that those methods were derived from the

24

earlier methods and earlier standards (i.e. the ASTM D 6391 (2009) and the ASTM D6391 (2009) Standards). Evaluations of these methods, and standards, were performed by Nanak (2012) and Blanchard (2013) to evaluate the accuracy and efficiency of each method proposed in the ASTM D6391 (2011) standard, the results of which are summarized herein.

3.7. Methods and Procedures

3.7.1. Testing Program

A series of laboratory tests were performed on field-scale test pads within the laboratory. TSB tests were performed on Test Pad 1, Test Pad 2, and Test Pad 5 and were used to evaluate the methods proposed in ASTM D6391 (2011). Sealed Double Ring Infiltrometer (SDRI) tests, which are also commonly utilized to determine hydraulic conductivity, were performed on Test Pads 3 and 4 and were used to evaluate the methods proposed in ASTM D5093 (2015).

As discussed in Maldonado and Coffman (2012), Test Pad 1 was additionally utilized to verify that results obtained from the constructed laboratory test pad were comparable to results obtained from a field test pad using the same soil. Discussion and results contained herein will focus primarily on Test Pads 1, 2, and 5. The results of Test Pads 3 and 4 are presented only for the purpose of validation and comparison because a TSB test was not performed within these pads.

3.7.2. Test Pad Construction and Testing

To evaluate the various methodologies for the TSB data reduction, the methodologies were analyzed for accuracy and efficiency. To facilitate this analysis, a test pad box was constructed at the atmospherically controlled UofA Engineering Research Center (ERC). The test pad box was a 3m-wide by 3m-long by 0.9m-deep square wooden box, constructed from timbers and braced by rakers. Furthermore, the bottom of the box was lined with a 0.15m-thick

25

pea gravel drainage layer (piezometric line) that was covered with a sheet of geotextile, and the sides of the box were lined with plastic sheets. The test pad box was constructed so as to be in compliance with the area constraints outlined in ASTM D6391 (2011) and ASTM D5093 (2015). A schematic of the test pad box is presented in Figure 3.2.
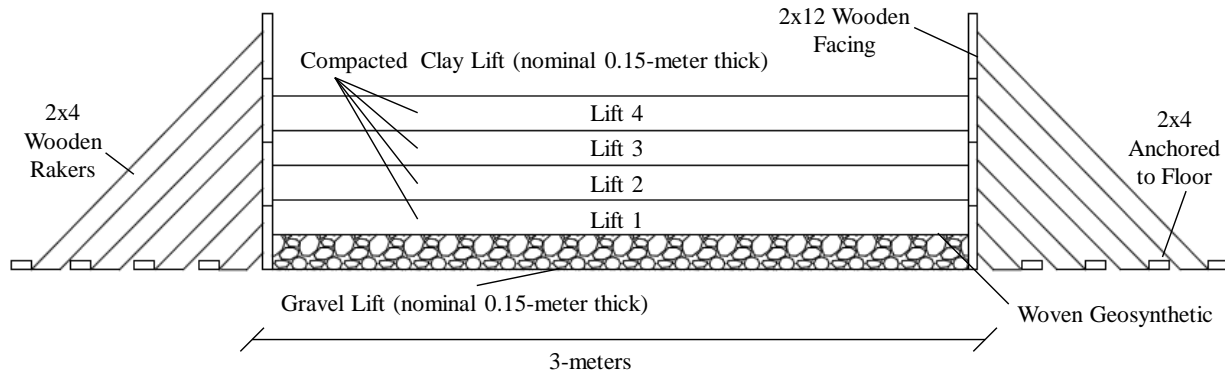
Figure 3.2. Dimensions of test pad box, modified from (Nanak, 2012).

The soil utilized in this testing program was identified as Northwest Arkansas "Red Dirt". Red Dirt was selected because of its availability in Northwest Arkansas and because this material has been utilized as a landfill liner at the nearby Eco-Vista Landfill. The results of soil index testing, reported in Nanak (2012), classified the Reddirt as a lean clay (CL) consisting of 87.5 percent fines, with a clay fraction of 27.3 percent, a liquid limit of 36, and a plastic limit of 17. The soil was stockpiled outside of the ERC and covered with a geosynthetic cover when not being used within a given test pad. Following deconstruction of each test pad, the soil from each test pad was placed back into the stockpile for reuse in future test pads. During the construction of each test pad, the soil was brought into the ERC using a tractor with a back-hoe attachment, a fork lift, and soil bags.

Test Pads 1, 2, and 5 were constructed utilizing similar construction procedures. However, there were variations in the Test Pad 5 construction procedure, which were associated with the procedures to facilitate in-situ instrumentation. For each test pad, four 0.15m-thick

26

compacted lifts were utilized to construct a 0.6-m thick compacted clay liner, which is a typical thickness utilized for landfill liners and covers. The thickness of each loose lift was verified using a tripod mounted automatic level and a level rod. The loose elevations were measured at each corner and at the center of the box for each lift.

Following placement of the loose lift, compaction of the clay liner was achieved using a Wacker BS700 gasoline powered rammer (Figure 3.3). For each lift, two passes were made with the compactor to achieve the aforementioned 0.15m-thick nominal compacted lift thickness. Any area that was not well compacted by the compactor (sides and corners of the box as well as directly over in-situ instrumentation in Test Pad 5) was compacted with a 0.2m by 0.2m square manual tamper. For each pass, compaction started in an outer corner of the test pad and progressed in a spiral pattern towards the center of the pad. Similar to the loose elevations, the compacted elevations were measured at each corner and at the center of the box for each lift.

(a)   (b)
Figure 3.3. (a) Manual tamper on center of pad, (b) Wacker near the center of pad.

Test Pad 5 was compacted to facilitate the installation of in-situ instrumentation; however, the aforementioned compaction methods that were utilized for Test Pad 1 and 2 were followed as closely as possible. Time Domain Reflectometry (TDR) probes and Water Matric Potential (WMP) sensors were installed within Test Pad 5 to monitor the volumetric water content and soil suction during TSB testing as part of an investigation of the Soil Water

27

Characteristic Curve (SWCC) that was described in Ishimwe (2014). One TDR probe and one WMP sensor were installed 0.05m below the top of Lift 1 and Lift 2 and three of each type of sensor were installed in Layer 4, with sensor heights above the base of Layer 4 being 0.05m, 0.10m, and 0.15m. A total of five TDR probes and five WMP sensors were used within Test Pad 5. To facilitate the placement of multiple sensors within Lift 4, Lift 3 and 4 were divided into two sub-lifts. Each sub-lift was comprised of a 0.1m-thick loose lift that was compacted with one-half of the compaction effort than what was utilized for a regular 0.2m-thick loose lift (one pass of the ramming compactor instead of two passes).

To ensure that the results of hydraulic conductivity testing were comparable between the different test pads, a zone of acceptance was developed and used as an acceptance criterion for each soil layer. The zone of acceptance (ZOA) was developed by Nanak (2012) and utilized the method described in Daniel and Benson (1990). This ZOA was constructed to bound all the acceptable values ($1x10^{-7}$ cm/s or less) for hydraulic conductivity and was constructed by conducting Flexible Wall Permeameter (FWP) testing on 18 Proctor samples compacted at various energies (Maldonado and Coffman, 2012). In accordance with ASTM D6938 (2017), each compacted layer within a given test pad, was tested using a Nuclear Density Gauge (NDG), to verify compliance with the ZOA. The results of the NDG testing are presented in Figure 3.4. As displayed in Figure 3.4c, the majority of points tested in Test Pad 5 plotted outside the ZOA; however, these layers were not removed and recompacted due to the presence of the in-situ instrumentation and the desire for measurement of the wetting curve. Consequently, Test Pad 5 was placed drier and at a greater density than Test Pads 1 and 2, which tested within the ZOA (with the exception of Lift 4 for Test Pad 1 which was also placed at a greater density).

28

After each test pad was compacted, a TSB and a Temperature Effects Gauge (TEG) were installed into each pad in accordance to ASTM D6391 (2011). Although each test pad was installed with a TEG, a malfunction in the Test Pad 5 TEG, which caused a continuous drop in the water level within the TEG, led to the Test Pad 5 TEG data being disregarded. However, because the laboratory was atmospherically controlled, the effects of temperature fluctuations between readings should be negligible. Additionally, during hydraulic conductivity testing, the test pad was covered with a plastic sheet to prevent the test pad from drying out. Preventing the test pad from drying out mitigated the possible effects from 1) desiccation and 2) change in soil suction from non-testing related changes in moisture content as observed in in-situ instrumentation in Test Pad 5. The variance in measured volumetric moisture content and pressure head in Layer 1, which was unaffected by TSB infiltration, was 32.96 to 31.98 percent and 0.29 cm to 0.82 cm, respectively. The typical cross-section of a nominal test pad is presented in Figure 3.5.

(c)
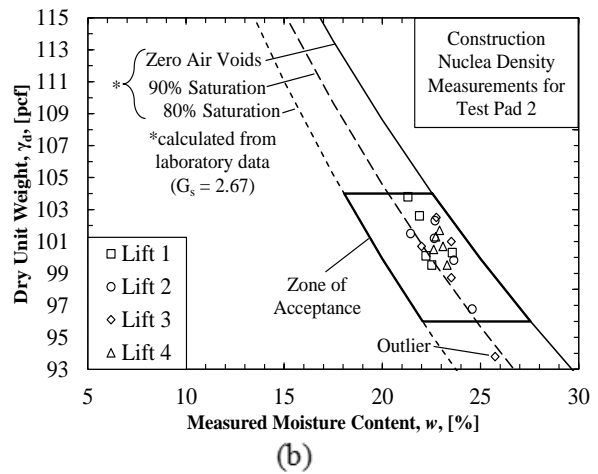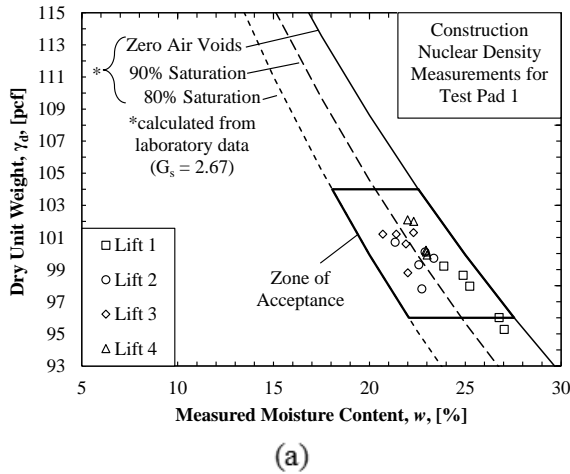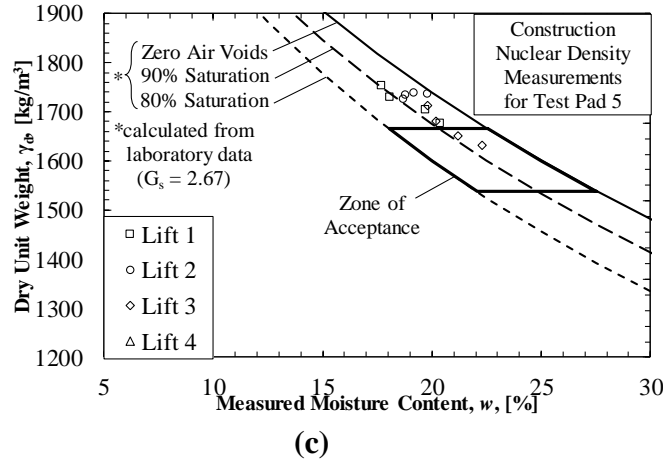
Figure 3.4. Results of nuclear density gauge plotted against the zone of acceptance for (a) Test Pad 1 (Nanak, 2012), (b) Test Pad 2 (Nanak, 2012), and (c) Test Pad 5 (Blanchard, 2015).
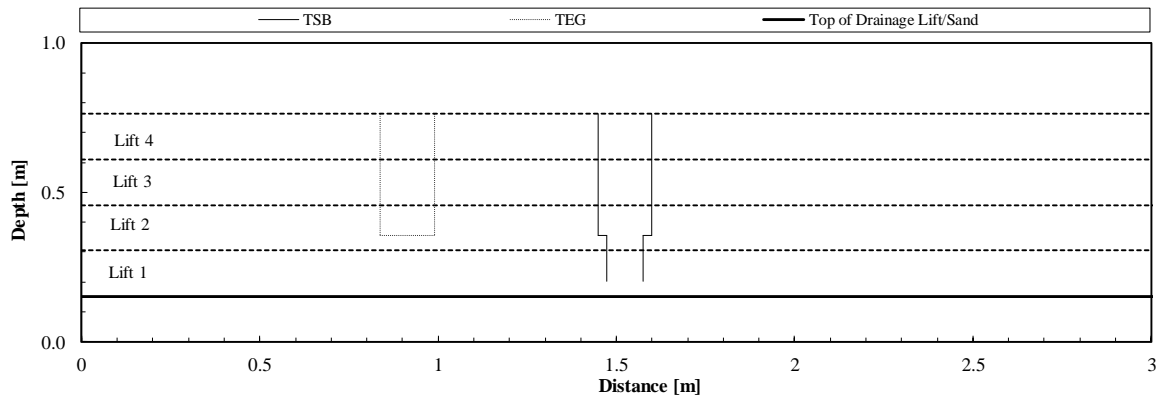
Figure 3.5. Typical profile view of test pad.

Following installation, Stage 1 testing was conducted using the TSB until the hydraulic conductivity reached a steady state of flow (equilibrium). Because Test Pads 1 and 2 were performed prior to the release of the ASTM D6391-11 standard, Test Pads 1 and 2 were tested using the falling head test methods (Method A and Method B). Conversely during Stage 1 of Test Pad 5, testing was performed using the constant head test method (Method C) and then the falling head test methods (Method A and Method B). This method of testing was achieved by first utilizing a standpipe with a Mariotte tube and then switching to a standpipe without a Mariotte tube after steady state flow had been achieved. Following Stage 1 testing, the standpipes were removed, the borehole was extended below the casing, the standpipes were

30

reattached, and Stage 2 testing was conducted. Stage 2 testing was completed using a falling head standpipe for each test pad because only Method A, which is a falling head test method, utilized Stage 2.

Testing procedures were held constant throughout the investigation. A maximum water height within the standpipe of 15 centimeters was used to limit the potential for hydraulic fracturing of the soil and to ensure similar pressure gradients were utilized during the various tests. However, the changes within the effective stress values, as caused by changes in the head level, affected the measured values of the hydraulic conductivity of the soil. Therefore, the results of a constant head test and a falling head test might not be in reference to the same value of total head, and therefore might have different measured values of hydraulic conductivity.

The hydraulic conductivity for falling head testing was evaluated utilizing the previously presented equations for Method A and B of ASTM D6391 (2011). Conversely, the hydraulic conductivity for constant head testing was evaluated for each time step using a modified form of Equation 3.12. The modified form (Equation 3.17), as derived herein (Equations 3.17 through 3.20), represents a correction to the Method C equation that is presented in the ASTM D6391 (2011) standard. Specifically, Equation 3.17 includes a factor of 4 that was not accounted for in the Method C equation. The results obtained from each time step, by utilizing either Method A, B, or C were averaged using a time weighted average, as recommended in ASTM D6391 (2011). Therefore, only data that were collected after the test had reached a state of temporal invariance (equilibrium) were considered. The resulting averages are presented and discussed within the next section.

$$k = R_t \frac{\frac{\pi}{4}(d_s{}^2 - d_m{}^2)(Z_1 - Z_2)}{2.75D(k_b)(t_2 - t_1)} \qquad \text{(Modified ASTM D6391, 2011)} \qquad [3.17]$$

$$Q = CkH \qquad \text{(Hvorslev, 1951)} \qquad [3.18]$$

31

$$Q = \frac{AR}{\Delta t} \qquad \text{(Hvorslev, 1951)} \qquad [3.19]$$

$$C = 2.75D \qquad \text{(Hvorslev, 1951)} \qquad [3.20]$$

Therefore, $k = \frac{Q}{CH} = \frac{\frac{AR}{\Delta t}}{CH} = \frac{AR}{\Delta t CH} = R_t \frac{\frac{\pi}{4}(d_s{}^2 - d_m{}^2)(Z_1 - Z_2)}{2.75D(k_b)(t_2 - t_1)}$

In Equations 3.17 through 3.20, d_s is equal to the ID of the standpipe; d_m is equal to the outer diameter (OD) of the Mariotte tube; Z_1 is the height of the water in the standpipe at the beginning of the interval(s); Z_2 is the height of the water in the standpipe at the end of the interval(s); D is the ID of the casing; k_b is the total head acting on the soil ($k_b = H$); t_1 is the time at the beginning of the increment(s); t_2 is the time at the end of the increment(s); A is the effective area of the standpipe ($A = (\pi/4)(d_s{}^2 - d_m{}^2)$); and R is the change in height of water in the standpipe ($R = Z_1 - Z_2$).

     Each of the results obtained from Method A, B, or C were compared to understand how the results from each of the methods performed relative to one another. Laboratory FWP test results from Test Pads 1 and 2 were also used to evaluate the results obtained from Methods A, B, and C. The FWP testing was performed in accordance with ASTM D5084 (2016) Method C, on samples extracted from Shelby Tubes and Hand Carved Samples. Additionally, the FWP testing procedures and results were described in detail in Nanak (2012). Test Pad 5 underwent extreme desiccation, with visible desiccation cracks, following a drying cycle that was performed as part of the previously mentioned study about the SWCC. Therefore, laboratory testing was not performed on Test Pad 5, because the results of which would have yielded uncharacteristic results due to the significant change in the soil state during desiccation.

     The coefficient of variation (COV) was also computed for each test pad and method. The COV was calculated by dividing the standard deviation of the average temperature corrected value of hydraulic conductivity for data considered to be temporally invariant for each filling of the standpipe by the average of the same date set. The average value for each filling of the standpipe was used to allow comparison between Methods A and C with Method B, for which

32

hydraulic conductivity is determined utilizing all the data for each filling of the standpipe. For Test Pads 1 and 2 and Test Pad 5 Method C, six tests were considered to be temporally invariant. For Test Pad 5 Method A and Method B, eleven tests were considered temporally invariant.

3.7.3. Calibration of Data Sheets

After the TSB testing was completed, the data were processed using Microsoft Excel. To ensure that the obtained results were accurate and obtained using the proper methodology, the sample data provided within the ASTM D6391 (2011) standard were utilized to validate the excel sheets. Through the process of validating the Excel sheets, several errors were observed within the provided results within the ASTM D6391 (2011) standard. It was also noted that there was inconsistency between the notation used in the sample data sheets and notation used within ASTM D6391 (2011) methodology, as well as the errors within the data sheets. This inconsistency may confuse practitioners. Therefore, each of the sample data sheets was analyzed for errors, and the results are reported herein.

3.7.4 Comparison of Method A and B

Method A and B can be utilized to analyze the same data set, because both Method A and B are falling head test methods. Therefore, in addition to comparing the results from the testing program, Method A and B were also used to analyze the data from the Method A sample data sheet in the ASTM D6391 (2011) standard. A similar analysis was performed by Nanak (2012); however, Nanak (2012) incorrectly processed the data for the Chiasson (2005) and Method B. A corrected comparison was performed and is presented herein.

33

3.8. Results and Discussion

3.8.1. TSB Testing

The results obtained during TSB testing for Methods A and B for Test Pads 1, 2, and 5, are presented in Figure 3.6a, 3.6b, and 3.6c, respectively. For completeness, final results from each test pad and from each method, as well as the results from FWP tests conducted on samples taken from Test Pads 1 and 2, are presented in Table 1.
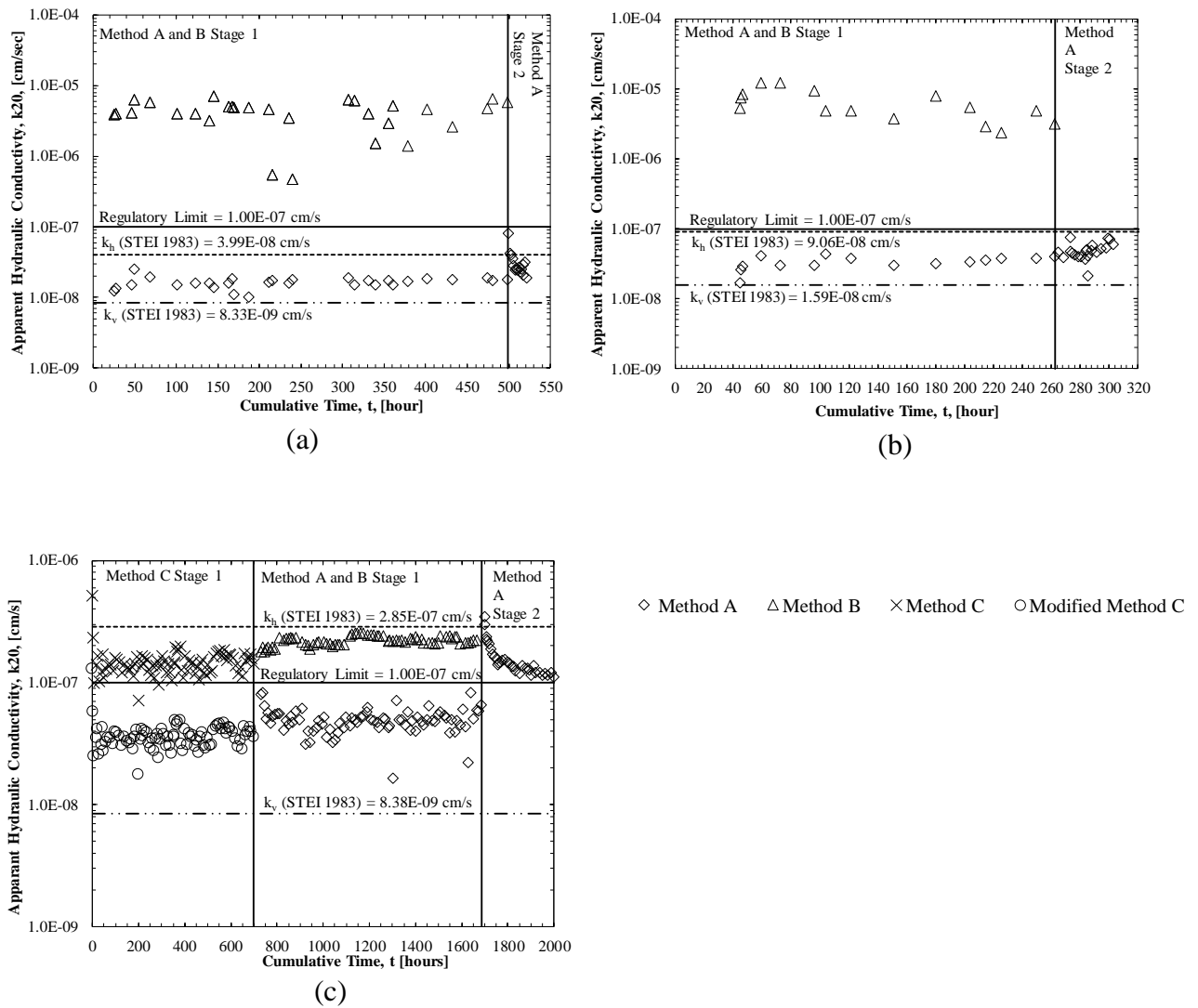
Figure 3.6. Results of in-situ hydraulic conductivity testing for (a) Test Pad 1, (b) Test Pad 2, and (c) Test Pad 5.

Table 3.1. Results of hydraulic conductivity testing for Test Pad 1, 2, and 5.

Average	Method	Test Pad 1 [cm/s]	Test Pad 2 [cm/s]	Test Pad 5 [cm/s]	Average COV for Each Method
K1	A	1.09E-08	2.18E-08	4.88E-08	0.066
K2	A	1.50E-08	3.13E-08	1.19E-07	0.010
k_{v20}	A	5.13E-09	9.41E-09	8.38E-09	--
k_{h20}	A	2.52E-08	5.51E-08	2.85E-07	--
k_{20}	B	4.38E-06	4.47E-06	2.25E-07	0.316
k_{20}	C	--	--	1.43E-07	0.056
k_{20}	$C_{corrected}$	--	--	3.58E-08	0.056
k_{20}	Lab	7.32E-08	3.67E-08	--	--

Within Test Pads 1 and 2, the average value of the laboratory-obtained FWP results (7.32E-08cm/s and 3.67E-08cm/s, respectively) were in relative agreement, within one order of magnitude, with the average value of results that were obtained by utilizing Method A during Stage 1 of testing (1.09E-08cm/s and 2.18E-08cm/s, respectively). In contrast, the results that were obtained utilizing Method B were almost two orders of magnitude greater than the results obtained from Method A or from the laboratory FWP. Although no laboratory testing was performed on Test Pad 5, the values obtained during in-situ testing should be very similar to the values obtained during Test Pad 1 and 2 testing.

As expected, the average value obtained utilizing Method A during Stage 1 for testing performed on Test Pad 5 (4.88E-08cm/s) was very similar to the average value obtained utilizing Method A for testing performed during Stage 1 on Test Pads 1 and 2; the results were within one-half of an order of magnitude. Additionally, the measured vertical hydraulic conductivity values for Test Pad 1, 2, and 5 were also very comparable (5.13E-9cm/s, 9.41E-08cm/s, and 8.38E-09cm/s, respectively). In contrast, the average value obtained by utilizing Method B (2.25E-07cm/s) and Method C (1.43E-07cm/s), from the ASTM D6391 (2011), during Stage 1

35

for Test Pad 5 were higher than the average value obtained by utilizing Method A, by almost a full order of magnitude (as seen in Figure 3.6c). However, it should be noted that the average value obtained by using Method B is a full order of magnitude closer to the results obtained from Method A for the Test Pad 5 data, as compared to Test Pad 1 and 2 data. Additionally, the average value obtained from Method C, as obtained using the corrected Equation 3.17 (3.58E-08cm/s), was very similar to average value obtained by utilizing Method A for the Test Pad 5 data.

The consistent results obtained from Method A between Test Pad 1, 2, and 5 as well as the supporting results obtained from the laboratory FWP and the corrected Method C values (all values being within one order of magnitude) suggest that these methods produce the most representative results. Additionally, because the results obtained from Method B were consistently above the consensus values, Method B is believed to be overly conservative for landfill liner applications. However, as previously noted, the accuracy of Method B was significantly improved during the testing performed on Test Pad 5. This was attributed to an increase in the number of readings taken during each filling of the standpipe during testing within Test Pad 5 (8.5 readings on average) as compared to number of readings taken within Test Pads 1 and 2 (2.2 readings on average).

The increased number of readings per filling of the standpipe is an important factor in Method B because the value of "a" is determined via an iterative process based on the results of each time step (reading). The iterative process was developed by Chiasson (2005) to reduce the effects caused by "inaccuracies in measurements" which were amplified via the problem of double inaccuracies in derivatives while utilizing the velocity method that was proposed by Chapius (1999). However, the iterative process is dependent upon having sufficient data points

to create meaningful boundary conditions that produce a significant solution to mitigate the inaccuracies within the velocity method. No guidance is provided within ASTM D6391 (2011) or within Chiasson (2005) regarding the recommended number of readings to perform Method B testing.

A lack of meaningful boundary conditions creates the potential that Method B analysis will be under constrained. Method B utilizes three variables (a, Z^*, and Z_o), but only has two constraining conditions (Equations 3.14 and 3.15). Utilizing three variables is a variation of the velocity method proposed by Chapuis (1999) which determined Z^* directly from the y-intercept of the velocity graph. Method B being under constrained would explain why increasing the number of readings improves accuracy, because increasing the number of readings strengthens both constraining conditions. However, a third constraint maybe needed to correct for the existing deficiencies in Method B.

The increased number of readings also increased the consistency of the results that were obtained using Method B as was evident by the decreased value of the coefficient of variation (COV). The average value of the COV for Method B data in Test Pad 1 and Test Pad 2 was 0.439, while the COV for Method B data in Test Pad 5 was 0.056. The continued over estimation of the value of hydraulic conductivity, even with the decrease in the value of COV, for Test Pad 5, suggests that although a sufficient number of data points were available, Method B still did not produce consensus results. Additional discretization (increased number of readings per standpipe filling) may continue to enhance the accuracy obtained from the Method B analysis, but further investigation is required to draw any definitive conclusions.

Utilizing the in-situ instrumentation within Test Pad 5, it is also possible to evaluate Method B's ability to correct for the location of the Piezometric Line. Although the piezometric

37

line is believed to be located at the drainage layer, rather than making that assumption, the WMP probes allow for direct calculation of the pressure head. The pressure head corresponds to the difference between the assumed and the true location of piezometric line (Z^*). The low value of Z_o determined from in-situ instrumentation (0.6 cm), for a representative fill of the standpipe, was over an order of magnitude less than the value of Z^* determined utilizing Method B (8.2 cm). The low value of Z^* determined from the in-situ instrumentation indicates that the assumed location of the piezometric line was reasonable. By substituting the value of Z^*, determined from in-situ instrumentation, for the value of Z^* in Method B, the value of hydraulic conductivity that was determined (5.26E-08 cm/s) was within one order of magnitude of Method A and the corrected Method C in Test Pad 5. The comparison of in-situ and Method B determined values of Z^* demonstrates that Method B is an inaccurate way of determining Z^* (further evidence that Method B is under constrained).

As previously mentioned, the results obtained from the corrected Method C analysis are in relative agreement with the results obtained from the Method A analysis and from the results obtained from FWP testing. This provides additional validation for Equation 3.17. Consequently, it was concluded that the corrected Method C (Equation 3.17) provided more representative values of hydraulic conductivity for the compacted clay liner.

The average value of hydraulic conductivity that was obtained by using Method A, during Stage 2 (K2) of the test performed on Test Pad 5 (1.19E-07cm/s) was approximately one order of magnitude higher than the hydraulic conductivity values that were obtained by Nanak (2012) for Test Pad 1(1.50E-08cm/s) and Test Pad 2 (3.13E-08cm/s). This disparity was in part attributed to the drier placement in Test Pad 5, and was also attributed to the introduction of half lifts that were utilized for the installation of the probes into Test Pad 5. The value for horizontal

38

hydraulic conductivity obtained using the anisotropy (m) value for Test Pad 5 (2.85E-07 cm/s) was also approximately one order of magnitude greater than the same values calculated for Test Pad 1(2.52E-08 cm/s) and Test Pad 2 (5.51E-08 cm/s).

3.8.2. Calibration of Data Sheets

Due to errors within the ASTM D6391 (2011) data sheets, discrepancies were encountered during the process of validation of the data sheets. A subsequent review of the provided sheets helped to identify the errors, which are reported herein. During the review of the example data sheets, errors were discovered in both the Method A and Method B data sheets.

Many of the errors in the Method A data sheet were relatively trivial, and can be attributed to rounding errors. Specifically, during Stage 1, 1) the first three temperature correction factors, 2) the first two values of K1 and 3) the fourth value of K1 were reported as 0.01 lower than was appropriate (they were rounded down rather than up). Similarly, during Stage 2 the second, fourth, and fifth value of the temperature correction factor were also rounded down rather than up. However, the errors in the K2 calculations were more significant. In addition to the third value of K2 being off by a value of 0.01, and the final two values of K2 being off by a value of 0.02, the values reported did not correspond with the reported calculated values of G2 and G3. The G2 and G3 terms were calculated using a value of zero for the "a" term (from Method A). An "a" term of zero corresponds to an infinite medium ($b_1 > 20D$); however, that was not consistent with the reported data. Based upon the reported data, "a" should have equaled a value of negative one, which corresponds to the reported values for K2. Finally, the calculated values of cumulative volume could not be replicated, it was unclear what error occurred.

39

Because the exact process used to solve for the results reported in the Method B data sheet is unknown, it was difficult to identify errors within data sheet. However, several inconsistencies within the data sheet were identified. It was determined that the reported parameters (a, Z^*, and Z_o) do not correspond with the reported "Z-t Computations". When utilizing the reported parameters, the sum of the difference between observed and calculated values of Z (Equation 3.15) was not equal to zero ($-4.345m^2$), nor was the expression presented as Equation 3.14 minimized by the reported parameters ($0.385m$). In fact, using the Solver tool within an Excel sheet, along with the reported parameters as initial inputs, the data were reanalyzed and values of $7.85E-07m^2$ and $3.98E-04m$ were obtained for Equation 3.14 and 3.15, respectively, which are more reasonable values. The reported value of hydraulic conductivity was $7.99E-05m/s$; however, after the data was reanalyzed a value of $2.54E-04m/s$ was obtained for the soil hydraulic conductivity. This value is over a full order of magnitude larger than the reported hydraulic conductivity value.

A review of the Method C data sheet was also performed, but no errors were found. However, the data sheet did not utilize the equation for Method C as written, but rather the flow area was determined directly and inserted into Equation 3.19. Consequently, the error within the Method C equation was avoided.

The inconsistency and errors within the data sheet may be confusing to data analyzers. Additionally, the change in terminology between ASTM D6391 (2011) and the data sheets may also be another source of potential error. Errors should be addressed in future revisions of the ASTM D6391 standard to reduce the possibility of calculation errors by practitioners.

3.8.3. Comparison of Method A and B

The data set provided in the Method A data sheet was analyzed using Method B in order to compare the performance of the two methods. The results support previously identified trends during TSB testing. The average value of hydraulic conductivity that was obtained by utilizing Method B was 4.54E-06cm/s, or about one half of one order of magnitude less than the average value of hydraulic conductivity that was obtained by utilizing Method A (9.36E-07cm/s). This comparison provides further validation of the discrepancy between the two methods. In every data set that was analyzed by the two methods during this investigation, the results obtained from Method B were higher in magnitude than the results obtained from Method A.

This is consistent with the results obtained by Nanak (2012); however, as previously mentioned, the results presented in Nanak (2012) also contained an error. During the process of unit conversion, Nanak (2012) divided minutes by 24 while converting to seconds, which was incorrect. Nanak (2012) also proposed a unit specific equation for Method B; however, that is not a recommended practice because practitioners may not realize that the equation is unit specific and mistakenly use other units. Rather the preferred practice is for practitioners to rely upon dimensional analysis to determine appropriate units.

3.9. Conclusions and Recommendations

An investigation into the methods utilized for determining hydraulic conductivity of compacted clay liners was performed. Specifically, the methods utilized in the analysis of TSB testing data, as permitted within the ASTM D6391 (2011) standard, were evaluated. The investigation consisted of 1) reviewing the evolution of the equations that were used for TSB analyses, 2) a testing program where each method was used to evaluate the hydraulic conductivity of a laboratory compacted clay liner, and 3) validation of the obtained field results

41

through the use of laboratory FWP testing. During the course of this investigation, several conclusions and recommendations were derived.

- The equation utilized in Method C (Equation 3.12) was derived incorrectly. Equation 3.17, as reported herein, represents the correctly derived Method C equation. This is supported by mathematical derivation and empirical results. Therefore, it is recommended that Equation 3.17 be used when performing Method C analysis.

- The results obtained utilizing Method A and the modified Method C for analysis are in relative agreement with one another and with laboratory-obtained FWP results; however less variability was observed in Method C.

- Method B is highly dependent on the number of time steps (data readings) used during each emptying of the standpipe. This phenomenon should be investigated further and guidelines should be published for number of readings required per filling/emptying of the standpipe. It is anticipated, that approximately 10 or more readings may be needed to obtain sufficient accuracy. This may limit the applicability of Method B as data are commonly collected on an as available basis.

- It is recommended that until guidelines for the required number of readings per emptying of the standpipe be employed to obtain consistently accurate results, Method B not be utilized for landfill liner regulation applications.

- Method B is overly conservative for landfill applications. For each data set analyzed herein, the results obtained from Method B were significantly (one half to two orders of magnitude) greater than the results obtained from the other methods.

- Method B, as presented in ASTM D6391 (2011), may be under constrained and is not recommended for use in its current form. However, by directly solving for the variable

42

Z*, a representative value of hydraulic conductivity was determined. Therefore, if Method B is utilized, the location of the piezometric line should be verified using additional means.

- The ASTM D6391-11 standards contain several errors in the example data sheets that may be confusing. These errors must be fixed before the next standard issuance.

3.10. References

ASTM (2016), "Standard Test Method for Measurement of Hydraulic Conductivity of Saturated Porous Materials Using a Flexible Wall Permeameter," Annual Book of ASTM Standards, Designation D 5084, Vol. 4.08, ASTM, West Conshohocken, PA.

ASTM (2015), "Standard Test Method for Field Measurement of Infiltration Rate Using Double-Ring Infiltrometer with Sealed-Inner Ring" Annual Book of ASTM Standards, Designation D 5093, Vol. 4.08, ASTM, West Conshohocken, PA.

ASTM (2011), "Standard Test Method for Field Measurement of Hydraulic Conductivity Using Borehole Infiltration" Annual Book of ASTM Standards, Designation D 6391-11, Vol. 4.08, ASTM, West Conshohocken, PA.

ASTM (1999), "Standard Test Method for Field Measurement of Hydraulic Conductivity Limits of Porous Materials Using Two Stages of Infiltration from a Borehole" Annual Book of ASTM Standards, Designation D 6391-99, Vol. 4.08, ASTM, West Conshohocken, PA.
ASTM (2006), "Standard Test Method for Field Measurement of Hydraulic Conductivity Limits of Porous Materials Using Two Stages of Infiltration from a Borehole" Annual Book of ASTM Standards, Designation D 6391-06, Vol. 4.08, ASTM, West Conshohocken, PA.

ASTM (2017), "Standard Test Method for In-Place Density and Water Content of Soil and Soil-Aggregate by Nuclear Methods (Shallow Depth)," Annual Book of ASTM Standards, Designation D 6938, Vol. 4.08, ASTM, West Conshohocken, PA.

Blanchard, J, (2015). Evaluation of the Equations Used to Calculate Hydraulic Conductivity Values From Two-Stage Borehole Tests, *Honors Thesis*, University of Arkansas, May 2015

Boutwell, G., (1992). "The STEI Two-Stage Borehole Field Permeability Test." Containment Liner Technology and Subtitle D, Houston Section, ASCE, Houston, TX.

Boutwell, G. and Tsai, C., (1992). "The Two-Stage Field Permeability Test for Clay Liners." *Geotechnical News*, C. Shackelford and D. Daniel, eds., pp. 32-34.

Chapuis, R., (1999). "Borehole Variable-Head Permeability Tests in Compacted Clay Liners and Covers." *Canadian Geotechnical Journal*, Vol. 36, pp. 39-51.

Chiasson, P., (2005). "Methods of interpretation of borehole falling-head tests performed in compacted clay liners." *Canadian Geotechnical Journal*, Vol. 42, pp. 79-90.

Daniel, D., (1989). "In Situ Hydraulic Conductivity Tests for Compacted Clay." *Journal of Geotechnical Engineering*., ASCE, Vol. 115, No. 9, pp. 1205-1226.

Daniel, D. and Benson, C., (1990). "Water Content-Density Criteria for Compacted Soil Liners." *Journal of Geotechnical Engineering*, ASCE, Vol. 116, No. 12, pp. 1811-1830.

Hvorslev, J., (1951). "Time Lag and Soil Permeability in Ground Water Observations." Bulletin No. 36, United States Army Corps of Engineers, Waterways Experiment Station, Vicksburg, MS.

Ishimwe, E, (2014). Field-Obtained Soil Water Characteristic Curves and Hydraulic Conductivity Functions. Masters Thesis, University of Arkansas, May 2013.

Nanak, M, (2013). Variability in the Hydraulic Conductivity of a Test Pad Liner System Using Different Testing Techniques. Masters Thesis, University of Arkansas, May 2013.

Maldonado, C., and Coffman, R., (2012). "Hydraulic Conductivity of Environmentally controlled Landfill Liner Test Pad." ASCE Geotechnical Special Publication No. 225, roc. GeoCongress 2012: State of the Art and Practice in Geotechnical Engineering, Oakland, California, March, pp. 3593-3602.

Soil Testing Engineers, Inc. (1983). *STEI Two-Stage Field Permeability Test*. Soil Testing Engineers, Inc., Baton Rouge, LA.

Trautwein, S. and Boutwell, G. (1994). "In situ hydraulic conductivity tests for compacted soil liners and caps." *Hydraulic Conductivity and Waste Contaminant Transport in Soil*, STP 1142, D. Daniel and S. Trautwein, eds., ASTM, Philadelphia, pp. 184-223.

45

CHAPTER 4: FIELD-OBTAINED SOIL WATER CHARACTERISTIC CURVES AND HYDRAULIC CONDUCTIVITY FUNCTIONS

4.1. Chapter Overview

The soil water characteristic curves (SWCCs) and hydraulic conductivity function (k-functions), as determined from field and laboratory settings, are compared and discussed in this chapter. Curves from field-scale tests were developed by utilizing in situ instrumentation. Five test pads were constructed at the University of Arkansas; however, this investigation only utilized data from two of the test pads. Specifically, Test Pad 4 and Test Pad 5 were used for this study. However, for the manuscript presented in this chapter the test pads were referred to as Test Pad 1 and Test Pad 2. Laboratory curves were obtained from laboratory tests performed on Shelby tube samples extracted from Test Pad 1. Specifically, the transient water release and imbibitions method (TRIM) and chilled mirror technique-based dewpoint potentiometer (WP4) method were utilized to determine the laboratory curves.

The limitations of the included accepted journal manuscript, that is presented in this chapter, are discussed in Section 3.2. The full citation for the manuscript is included in Section 4.3. Moreover, the motivation for the manuscript that is included in this chapter is discussed in Sections 4.4, 4.5, and 4.6. Descriptions of the methodologies and procedures for compacted clay liner construction, instrumentation, and testing are presented in Section 4.7. The results from the research are presented in Section 4.8; specifically, details from the field and laboratory hydraulic conductivity, in-situ instrumentation response, SWCCs and k-functions, measured and predicted hydraulic conductivity and flow, and effects of testing procedures are presented in Section 4.8.1, 4.8.2, 4.8.3, 4.8.4, and 4.8.5, respectively. Finally, conclusions about field-scale SWCCs and k-functions are presented in Section 3.9.

4.2. Limitations of the Described Study

The laboratory-determined SWCCs were only obtained from two of the common laboratory methods. Several other methods like: tempe cell, pressure plate extractor, centrifuge, and other laboratory methods that are commonly used to determine SWCCs were not considered. Additionally, the nature of the test pads (being placed wet of optimum) made the determination of the wetting SWCCs difficult. These aforementioned challenges are addressed in the manuscript by limiting discussion to the laboratory methods (TRIM and WP4) utilized in the study and selecting representative field curves that underwent greater changes in water content.

4.3. Field-Obtained Soil Water Characteristic Curves and Hydraulic Conductivity Functions

4.4. Abstract

A test program consisting of two, field-scale, compacted clay liners (test pads) was conducted to evaluate field-obtained soil water characteristic curves (SWCCs) and hydraulic conductivity functions (k-functions). The test pads were instrumented with volumetric water content and soil water matric potential sensors. Each test pad was subjected to an infiltration cycle, using either a sealed double ring or a two-stage borehole infiltrometer, followed by a drying cycle. To compare the results that were obtained from the field-obtained SWCCs and k-functions, laboratory tests were performed on Shelby tube samples. The obtained data were fitted using the van Genuchten model and the RETC (RETention Curve) program. A comparison of the results, as obtained from field-scale and laboratory techniques, was completed to illustrate the evidence of hysteresis between the drying and wetting curves. The shapes of the field and

47

laboratory-obtained SWCC were similar, albeit, at different volumetric water contents. There was poor agreement between field-obtained and laboratory-obtained k-functions, as reported in other studies; therefore, field k-functions are preferential when available.

Keywords: Unsaturated Soil Properties, Soil Water Characteristic Curve, SWCC, Hydraulic Conductivity Function, Hysteresis, Clay Liners, Landfills, Environmental and Waste Management.

4.5. Introduction

Soil water characteristic curves (SWCCs) and hydraulic conductivity functions (k-functions) have been useful in predicting the unsaturated properties of soils, including the values of: hydraulic conductivity, shear strength, and coefficients of diffusion and adsorption (Klute et al. 1986; Fredlund et al. 1994; Fredlund 1995; Fredlund and Rahardjo 1996; Fredlund et al. 1996; Fredlund and Xing 1997; Lu and Likos 2004; Lu and Kaya 2013). These two functions have been also used to evaluate the behavior of unsaturated soils (Fredlund and Rahardjo 1993). In addition, the SWCCs have been used to estimate water storage capacity of the soil subjected to various moisture content and suctions (Johari and Nejad 2015). This significant information can be used to aid in irrigation scheduling and to conserve irrigation water supplies. Improved irrigation efficiency can lead to reduced production costs for crops. As reported in Fredlund and Rahardjo (1993), many of the geotechnical engineering problems (e.g., slope, shallow and deep foundations failures following rainfall, swelling and shrinkage of clays) that occur in arid and semiarid climatic areas are associated with unsaturated soils. Therefore, a better understanding of the unsaturated soils behavior is necessary required while designing various geotechnical elements. The time and cost of the required soil testing to determine these unsaturated soil properties have been reduced by utilizing the SWCCs and k-functions. Like with other soil

48

phenomena (strength, permeability, compressibility), these characteristic functions have been typically measured in the laboratory (Wang and Benson 2004; Mijares and Khire 2010; Wyllace and Lu 2012; ASTM D6836 2008) with the results then being applied to determine the full-scale field responses. Although SWCCs have been frequently obtained by using laboratory equipment in the laboratory, few field measurements of SWCCs have been completed using field-testing equipment (Watson et al. 1975; Tzimas 1979; Li et al. 2004).

Two field-scale compacted clay liners were constructed and equipped with in-situ instruments to develop a field method to attain the SWCCs and k-functions. Each test pad was subjected to 1) a wetting cycle, using either a sealed double ring infiltrometer (SDRI) or a two-stage borehole (TSB) infiltrometer, and 2) a drying cycle. In-situ instrumentation was utilized to capture the changes in volumetric water content and matric suction that were required to assess the SWCC and k-function during each phase. Laboratory tests including: transient water release and imbibitions (TRIM), chilled mirror technique-based dewpoint potentiometer (WP4), and flexible wall permeability (FWP), were conducted, to develop laboratory SWCCs and k-functions, on Shelby tube samples that were collected after the drying cycle. The TRIM and WP4 tests are both commonly used methods for determining SWCCs and k-functions. The differences between the field and laboratory-obtained SWCCs and k-functions provide new insights on the validity of the methods used to obtain SWCCs and k-functions. The steps of this test program are summarized in the flowchart presented in Figure 4.1.
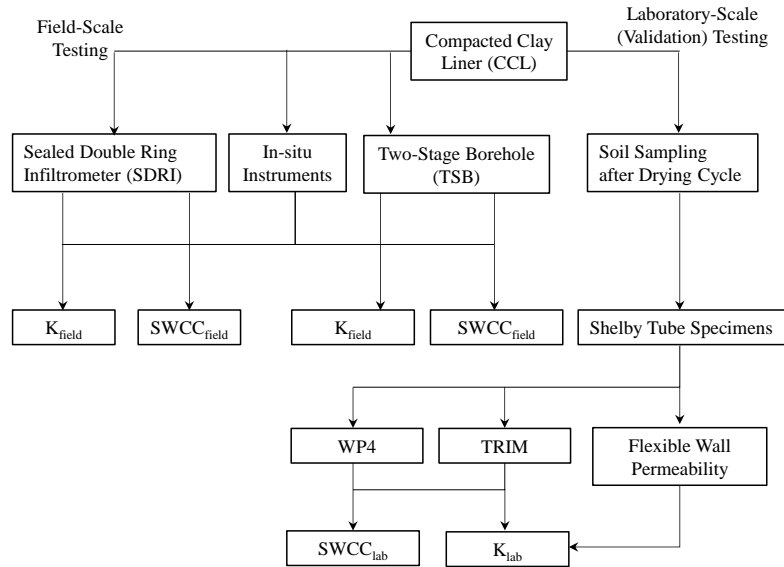
Figure 4.1. Flowchart of the testing program.

4.6. Background

The SWCC has become an important tool for predicting the mechanical and hydraulic

properties of unsaturated soils Fernando (2005). As documented within the literature, several

laboratory techniques exist for measuring the SWCC (Klute et al. 1986; Wang and Benson 2004;

Mijares and Khire 2010; Wayllace and Lu 2012; ASTM D 6836 2008). However, few field-scale

methods have been developed to determine SWCCs (Watson et al. 1975; Tzimas 1979; Li et al.

2004; Ogorzalek et al. 2008). Specifically, Watson et al. (1975) measured the field SWCC using

triangular pyramid frame housing instrumentation to determine the water content and

tensiometers to measure the soil water pressure required to obtain the SWCC. Li et al. (2004)

also measured the field SWCCs at the crest and berm of a large cut slope in Hong Kong using

the time domain reflectometry probes and vibrating wire tensiometers to measure water content

and soil suction, respectively. Likewise, Ogorzalek et al (2008) used time domain reflectometry

probes and thermal dissipation sensors to define the SWCC for a capillary barrier cover in

Polston, Montana.

50

According to Lu et al. (2014), the hydraulic conductivity of the soil is no longer thought of as a constant. Instead, the hydraulic conductivity is now typically portrayed as function of either the degree of saturation or the amount of suction (matric potential) within the soil. K-functions, which are defined as the relationship between hydraulic conductivity (k) and water content or suction, have commonly been determined in the laboratory using rigid- and flexible-wall permeameters with flow being controlled by surface infiltration/gravity drainage and by pumps, respectively (Meerdink et al. 1996; Lu and Likos 2004).

The equations [Equation 4.1 and 4.2] proposed by Daniel and Trautwein (1986) are commonly used for calculating the in-situ hydraulic conductivity value from SDRI test data. Three methods presented in Trautwein and Boutwell (1994) are also commonly utilized to determine the hydraulic gradient (*i*), as required to calculate hydraulic conductivity (k). These three methods include 1) the wetting front method (Equation 4.3), 2) the suction head method (Equation 4.4), and 3) the apparent hydraulic conductivity method (Equation 4.5). A detailed discussion of these equations was presented in Nanak [2012].

$$k = \frac{I}{i} F$$ (Daniel Trautwein, 1986) [4.1]

$$I = \frac{Q}{tA}$$ (Daniel Trautwein, 1986) [4.2]

$$i = \frac{H + Z_w}{Z_w}$$ (Nanak, 2012) [4.3]

$$i = \frac{H + Z_w + H_s}{Z_w}$$ (Nanak, 2012) [4.4]

$$i = \frac{H + Z}{Z}$$ (Nanak, 2012) [4.5]

Within Equations 4.1 through 4.5, I is the infiltration rate, Q is the volume of flow, t is the sub-test time duration, A is the area of infiltration, F is the correction factor to account for lateral spreading of water, H is the head of water above the soil surface, H_s is the suction head at the

location of the wetting front, Z_w is the depth of wetting front below the soil surface, and Z is the depth of the test pad.

Two different methods to determine the in-situ based hydraulic conductivity from TSB testing are described in ASTM D6391 (2006). These methods include 1) Method A (Equations 4.6 through 4.16), and 2) Method C (Equation 4.17). Method A, a falling head test that includes both stages of the TSB test is commonly used to obtain the maximum value for the vertical hydraulic conductivity (K1) and the minimum value for the horizontal hydraulic conductivity (K2). The actual value of the horizontal hydraulic conductivity (k_h) and the actual value of the vertical hydraulic conductivity (k_v) may also be determined using this method.

$$K1 = \frac{R_t G_1 \ln\left(\frac{Z_1}{Z_2}\right)}{(t_2 - t_1)}$$ (ASTM D6391, 2011) [4.6]

$$K2 = \frac{R_t G_2 \ln\left(\frac{Z_1}{Z_2}\right)}{(t_2 - t_1)}$$ (ASTM D6391, 2011) [4.7]

$$R_t = \frac{2.2902\left(0.9842^T\right)}{T^{0.1702}}$$ (ASTM D6391, 2011) [4.8]

$$G1 = \left(\frac{\pi d^2}{11D}\right)\left[1 + a\left(\frac{D}{4b_1}\right)\right]$$ (ASTM D6391, 2011) [4.9]

$$G2 = \left(\frac{d^2}{16FL}\right)G3$$ (ASTM D6391, 2011) [4.10]

$$G3 = 2\ln(G4) + a\ln(G5)$$ (ASTM D6391, 2011) [4.11]

$$G4 = \frac{L}{D} + \left[1 + \left(\frac{L}{D}\right)^2\right]^{1/2}$$ (ASTM D6391, 2011) [4.12]

52

$$G5 = \frac{\left[\dfrac{4b_2}{D} + \dfrac{L}{D}\right] + \left[1 + \left(\dfrac{4b_2}{D} + \dfrac{L}{D}\right)^2\right]^{1/2}}{\left[\dfrac{4b_2}{D} - \dfrac{L}{D}\right] + \left[1 + \left(\dfrac{4b_2}{D} - \dfrac{L}{D}\right)^2\right]^{1/2}}$$

(ASTM D6391, 2011) [4.13]

$$F = 1 - (0.5623)e^{-1.566\left(\frac{L}{D}\right)}$$

(ASTM D6391, 2011) [4.14]

$$\frac{K2'}{K1'} = m\frac{\ln\left[\dfrac{L}{D}\sqrt{1 + \left(\dfrac{L}{D}\right)^2}\right]}{\ln\left[\dfrac{mL}{D} + \sqrt{1 + \left(\dfrac{mL}{D}\right)^2}\right]}$$

(ASTM D6391, 2011) [4.15]

$$K1' = k_v m = \frac{k_h}{m}$$

(ASTM D6391, 2011) [4.16]

$$k = \frac{\dfrac{\pi}{4}\left(d_s^2 - d_m^2\right)\left(z_1 - z_2\right)}{2.75D\left(k_b\right)\left(t_2 - t_1\right)}$$

(Blanchard, 2015) [4.17]

In Equations 4.6 through 4.17, d is the internal diameter (ID) of the standpipe; D is the ID of the casing; b_1 is the thickness of the tested soil below the casing; Z_1 is the effective head at the beginning of the time increment; Z_2 is the effective head at the end of the time increment; t_1 is the time at the beginning of the increment(s); t_2 is the time at the end of the increment(s); b_2 is equal to $(b_1 - L/2)$; L is the length of the Stage 2 extension; a is 1 if the base at b_1 is impermeable, 0 for an infinite thickness, and -1 if the base at b_1 is permeable; $K1'$ is the time weighted average for the temporally invariant period for K1; $K2'$ is the time weighted average during the temporally invariant period for K2; m is determined by using Equation 13 and is solved for by using the Excel solver function; d_s is equal to the ID of the standpipe; d_m is equal to the outer diameter (OD) of the Mariotte tube; and k_b is the total head acting on the soil ($k_b = H$).

4.7. Methods and Procedures

4.7.1. Compacted Clay Liner Construction, Instrumentation, and Testing

Two 3 m-wide by 3 m-long by 0.6 m-thick test pads were constructed following the

standard specifications that are commonly used to construct clay liners for landfill applications.

The materials that were utilized consisted of clay soils which are commonly utilized for the

53

landfill liner and cover material at the Eco-Vista Landfill in Northwest Arkansas. Both test pads was constructed by compacting four layers of clay. Specifically, each soil layer of the test pad was placed as a 0.2 m-thick loose lift and then compacted, within the same wooden box that was described in Maldonado and Coffman (2012) and Nanak (2012), to a 0.15 m-thick compacted lift. The lift thicknesses and total thicknesses of the compacted clay liners were the same size as for a full-scale compacted clay liner for a typical landfill. However, due to size limitations within the laboratory, the soil was only compacted using a ramming compactor instead of a kneading compactor. Prior the soil placement, soil index testing, such as: specific gravity, hydrometer analyses, percentage passing the No. 200 (75-μm) sieve and Atterberg Limits testing, were performed to determine the soil parameters required to classify the soil (Maldonado and Coffman 2012).

Following compaction of each layer, two types of sensors were installed within each of the layers at the locations shown in Figure 4.2 to obtain field-scale SWCCSs and k-functions. Specifically, in Test Pad 1, two Campbell Scientific CS-610 30 cm-long time domain reflectometry (TDR) probes and two Campbell Scientific CS-229 heat dissipation water matric potential (WMP) sensors were installed horizontally 0.05 m below the top of each layer. The installation depth was selected to limit soil disturbance while providing adequate soil coverage. Prior to installation, each sensor was calibrated to the test pad soil as recommended by Campbell Scientific. The sensors were installed by excavating soil from the surface of each lift as shown in Figures 4.2a and 4.2b. For Test Pad 1, following compaction of the last layer, two sets of tensiometers were installed at depths of 0.13 m, 0.27 m, and 0.58 m (for a total of six tensiometers) to monitor only the wetting front movement during SDRI testing (Figure 4.2a).

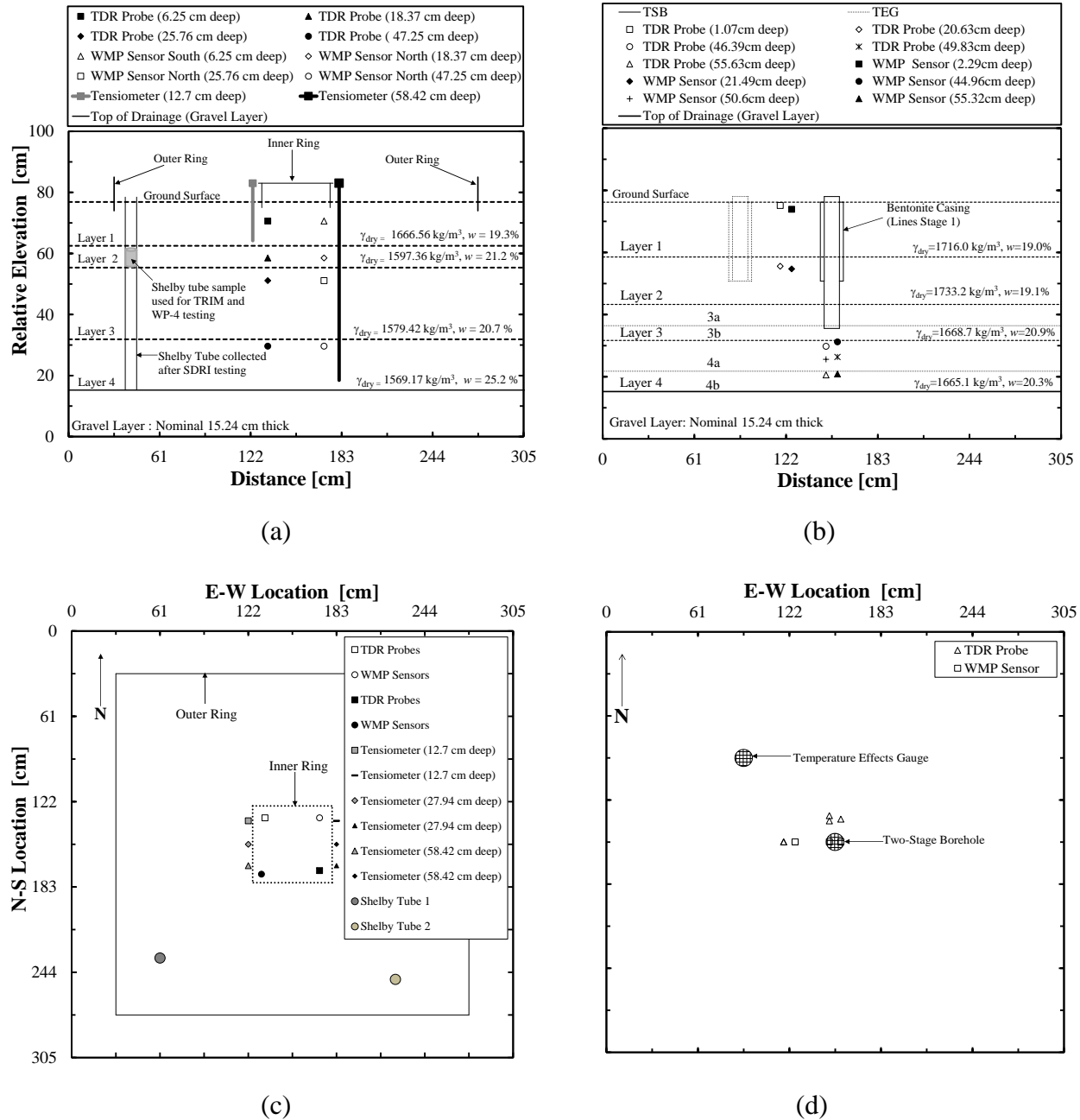**Figure 4.2.** Schematics of the instrumented compacted clay liners cross-section and plan view for (a, c) Test Pad 1; (b, d) Test Pad 2.

A sealed double ring infiltrometer with a square open outer ring (2.4 m by 2.4 m) and a square closed inner ring (0.46 m by 0.46 m) were then installed at the locations illustrated in Figures 4.2a and 4.2c. The SDRI was conducted in accordance with ASTM D5093 (2008).

Within Test Pad 2, a two-stage borehole (TSB) infiltrometer device was installed at the center of Test Pad 2 (Figure 4.2b and 4.2d). The data that were collected from the TDR probes and the WMP sensors were automatically monitored (hourly readings) using a computer that was connected to the data acquisition system.

Following the completion of test pad construction, in-situ hydraulic conductivity (SDRI or TSB) testing was conducted by following procedures outlined in Nanak (2012) and Blanchard (2015). Upon completion of the 69-days of SDRI testing, conducted within Test Pad 1, water was drained from both rings and the soil within the pad was allowed to undergo a drying cycle. The soil was allowed to dry for 86 days under an average temperature of 20ºC, with no direct sunlight, and no direct wind; desiccation cracks started to develop at the soil surface on the 14th day. The instrumentation within the compacted clay liner continued to collect continuous data during the drying cycle. Test Pad 2 underwent three phases of saturation; 1) the TSB testing or partial saturation phase, which lasted 81 days, 2) the saturation phase in which a soaker hose was used to saturate the entire compacted clay liner, which lasted 96 days, and 3) the drying/desaturation phase, which lasted 198 days.

The volumetric water content and water matric suction results that were obtained from the TDR probes and WMP sensors, were utilized to develop the field-scale SWCC. SWCC were developed for each depth that the sensors were located. The measurements acquired from the sensors were also used to determine the amount of time required for the wetting front to reach the location of each sensor. To obtain the laboratory-scale SWCCs and k-functions, the FWP, TRIM and WP4 devices were utilized to perform tests on sub-samples that were removed from one of the two Shelby tubes that were pushed into the soil of Test Pad 1. The TRIM method was performed at the Colorado School of Mines following the methods and procedures described in

56

Wayllace and Lu (2012). The chilled mirror hygrometer (WP4) method was performed at the University of Arkansas following the procedures described in Lin and Cerato (2012). In addition to the TRIM and WP4 laboratory tests, four flexible wall permeability (FWP) tests were also conducted in accordance with the ASTM D5084 (2010) Method C. Each of the FWP tests were terminated when a steady state hydraulic conductivity was achieved and when the outflow and inflow rate ranged from 0.75 to 1.25.

The experimental data, as obtained from 1) the in-situ instruments during SDRI and TSB testing (wetting cycle) and during the drying cycle, and 2) the WP4, were fitted to an existing parametric model using the RETC computer program. The van Genuchten hydrological parameters (α, m, n) that were measured from TRIM testing were utilized as initial values within the RETC program. The values for these parameters were then iterated, within the RETC program, using the van Genuchten (1991) parametric model and the Mualem (1976) theoretical pore-size distribution model to determine the SWCCs and k-functions for wetting and drying cycle, respectively. In addition, the HYDRUS-1D software was also utilized to estimate the movement of water through the soil. The SWCC parameters, and the FWP results were specified within the HYDRUS-1D model to estimate the required time for the wetting front to reach each sensor.

4.8. Results and Discussion

4.8.1. Field and Laboratory Hydraulic Conductivity

The in-situ hydraulic conductivity results that were collected immediately after compaction, by using the SDRI (Test Pad 1) and TSB (Test Pad 2) testing techniques, are presented in Figure 4.3a and 4.3b, respectively. As recommended in ASTM D5084 (2010), a typical plot of the hydraulic conductivity results as a function of cumulative pore volume of flow

57

(PV) of the samples collected from each layer of Test Pad 1 is presented as Figure 4.4. An average of the points, shown as open symbols in Figure 4.4, were considered as the final laboratory hydraulic conductivity of the soil. The FWP testing was not completed for Test Pad 4 because Test Pad 4 experienced severe desiccation making any subsequent laboratory testing unrepresentative. For comparison, the hydraulic conductivity obtained from the SDRI, the TSB and the FWP testing and the predicted values obtained using the RETC and HYDRUS-1D program are presented in Table 1. The obtained values were representative of the low plasticity clay (CL) soil with an average percent fines of 87.5 and 27.3 percent clay fraction with a specific gravity of 2.67 identified from index properties. A detailed discussion on index properties tests results is presented in Nanak (2012).

Table 4.1. Summary of measured and predicted hydraulic conductivity values.

	Measured k					Predicted k	
	SDRI			FWP	TSB	RETC	Hydrus-1D
	Wetting Front Method	Apparent Method	Suction Method	ASTM D5084 (Method C)	ASTM D6391 (Method A)	Mualem (1976)	van Genuchten (1980)
Layers	k_{20} (cm/sec)	k_{20} (cm/sec)	k_{20} (cm/sec)	k_{20} (cm/sec)	k_{20} (cm/sec)	k (cm/sec)	k (cm/sec)
Layer 1	1.04×10^{-07}	8.45×10^{-08}	9.27×10^{-08}	1.99×10^{-06}	-	5.86×10^{-07}	1.06×10^{-06}
Layer 2	4.54×10^{-07}	3.02×10^{-07}	4.32×10^{-07}	3.42×10^{-07}	4.88×10^{-08}	2.81×10^{-07}	1.26×10^{-06}
Layer 3	4.14×10^{-08}	5.47×10^{-08}	3.95×10^{-08}	2.17×10^{-08}	8.38×10^{-09}	1.33×10^{-07}	1.69×10^{-06}
Layer 4	-	-	-	4.66×10^{-08}	8.38×10^{-09}	2.26×10^{-07}	2.66×10^{-06}

58

Figure 4.3. Hydraulic conductivity results obtained from: a) SDRI, and b) TSB testing.
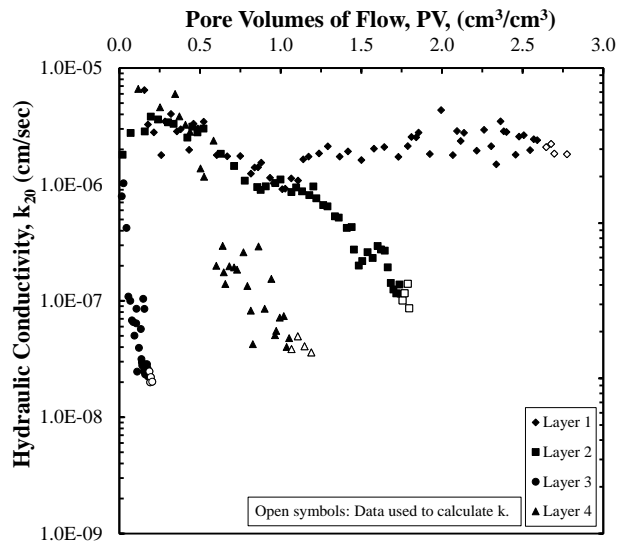
Figure 4.4. Laboratory vertical hydraulic conductivity results obtained from FWP testing within each layer.

The vertical hydraulic conductivity values that were obtained from the SDRI testing technique, by using the wetting front, apparent, and suction methods ranged from 0.27×10^{-7} to 4.5×10^{-7} cm/sec, while the values of laboratory hydraulic conductivity that were obtained from FWP testing technique ranged from 0.47×10^{-7} to 20×10^{-7} cm/sec. As expected, the hydraulic

59

conductivity values that were obtained from the FWP tests on soil that underwent a drying cycle, in which desiccation cracks formed, were higher than the field-obtained values of hydraulic conductivity that were obtained from the SDRI or TSB test. The average values for K1′ and K2′ that were obtained using Method A, for TSB testing, were 0.49×10^{-7} and 1.2×10^{-7} cm/sec, respectively. Additionally, the calculated k_v value was 0.084×10^{-7} cm/sec and the calculated k_h value was 2.9×10^{-7} cm/sec. Values obtained from Method A were reported previously in Table 1, with the K1′ value being reported as the hydraulic conductivity value for Layer 2 (the layer in which the Stage 1 testing was performed) and with the k_v value being reported as the hydraulic conductivity for Layers 3 and 4 (the layers in which Stage 2 testing was performed).

As previously mentioned, the soil compaction method was selected to ensure that the measured dry density and water content values were within the zone of acceptance (ZOA) (as developed by Maldonado and Coffman (2012) and reported in Nanak (2012), based on the procedures described in Daniel and Benson (1990)). For Test Pad 1, most of the tested points plotted within the ZOA, with the exception of Layer 4 (bottom of the pad), which was compacted dry of optimum (Figure 4.5). Conversely, for Test Pad 2, the tested points tended to be outside the ZOA due to greater density associated with over compaction. However, despite the points plotting outside the ZOA, the measured hydraulic conductivity values, that were obtained using the SDRI or TSB methods, were near the regulatory requirement of 1.0×10^{-7} cm/sec for a municipal solid waste landfill system.
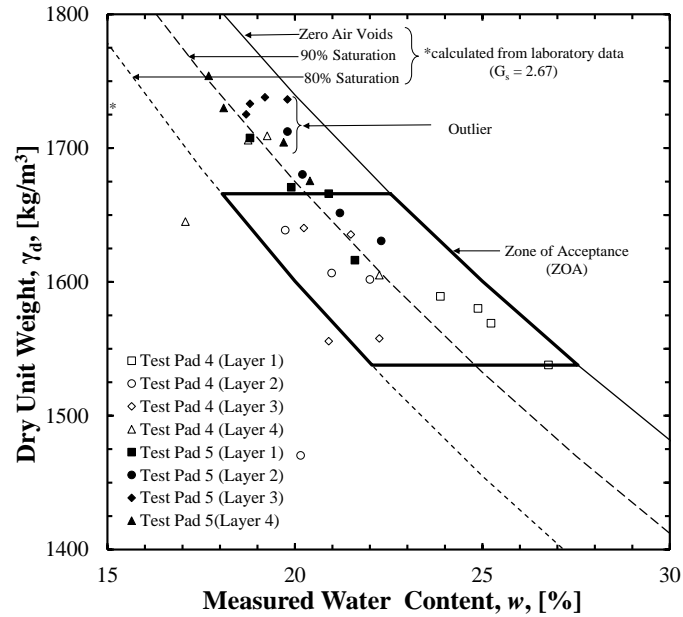
Figure 4.5. Nuclear gauge obtained in-situ density and water content values from Test Pads 1 and 2 overlaid on the zone of acceptance reported in Coffman and Maldonado (2012) and Nanak (2012).

As previously presented in Figure 4.3, the hydraulic conductivity results observed during the SDRI testing were closely correlated to the apparent values of hydraulic conductivity observed during Stage 1 TSB testing (within one-half order of magnitude). However, the resolved value for k_v from the TSB testing, as obtained by using Soil Testing Engineers Inc. procedures documented in STEI (1983), was one to two orders of magnitude less than the reported value from the SDRI testing. The difference between the two values was attributed to the variations in the soil density, water content values, and levels of macro-structure within the soil. Furthermore, the measured values of hydraulic conductivity for Test Pad 1, within each layer, were comparable to the predicted values that were obtained from the RETC and HYDRUS-1D programs, with values typically being within one order of magnitude. The measured values obtained from Test Pad 2 were less comparable to the predicted values of hydraulic conductivity, with values varying by as much as two orders of magnitude. The discrepancy between the predicted and measured values of hydraulic conductivity was attributed

61

to the predicted values being developed based only upon the in-situ data from Test Pad 2, Layer 1 (which had a lower saturated water content relative to the rest of Test Pad 2).

Layer 1 was utilized for the RETC and HYDRUS-1D analysis because it was reported to have the most clearly defined SWCC; this layer was placed drier than the other layers within both pads. Consequently, it was not necessarily representative of the initial conditions of the other layers. This observation of placement condition was supported by the measured in-situ data in both test pads (see Figures 4.6a and 4.6b). Even though Layer 1 of Test Pad 2 was the driest layer, in general, Test Pad 1 was tested drier than Test Pad 2 and correspondingly the measured SDRI and the predicted values were more comparable. The differences within the values of hydraulic conductivity, as obtained using the FWP, SDRI, and TSB devices were attributed to the following: 1) the SDRI and TSB was performed immediately after compaction and prior to the drying cycle, 2) the FWP was performed on soil that was subjected to the drying cycle (samples that were subjected to desiccation), 3) the cross-sectional areas of samples that were tested in the SDRI, TSB, and FWP tests were of different size and were therefore subjected to varying degrees of macrostructure, and 4) variances in the initial testing conditions.

4.8.2. In-situ Instrumentation Response

The time-dependent responses of the in-situ instrumentation that were located within Test Pad 1 and 2 are presented in Figures 4.6a and 4.6c and Figures 4.6b and 4.6d, respectively. As previously mentioned, these results were utilized for: 1) developing the field-obtained wetting and drying SWCCs and k-functions, and 2) identifying the amount of time required for the wetting front to reach the probes (during the infiltration phases). As observed in the response of all of the instrumentation, during the water infiltration, the TDR probes were not as sensitive to the changes in volumetric water content as the WMP sensors were to the changes in water matric

potential. In other words, because the soil was compacted on the wet side of the optimum water content, within the zone of acceptance, the expected increase of volumetric water content during the wetting cycle was not significant, as compared with the changes in volumetric water content that were observed during the drying cycle. Therefore, the variance in the probe sensitivity, observed in the response of the TDR probes, resulted in more clearly defined drying curves than wetting curves (Figures 4.6a and 4.6b).

Based on the results presented in Figure 4.6, the volumetric water content decreased and the water matric potential increased (became more negative) as a result of evaporation. The amount of time required for the wetting front to reach each WMP sensor was determined by identifying the time at which the probes reached a steady maximum value (with maximum value meaning smallest negative value). Ideally, the maximum value of water matric suction for each probes would have been 0 kPa. However, the maximum value of water matric potential for WMP sensors was-10 kPa, and as the recorded water matric suction approached -10 kPa; the wetting front was reported to have infiltrated to the depth of that sensor. Utilizing the TDR data, the wetting front was considered to have reached the respective TDR probes when the maximum volumetric water content was observed to have reached the respective probe. Within Test Pad 1, the WMP sensor performed better than the tensiometers for recording water matric potential (soil suction) values during the drying cycle because the tensiometer probes decoupled from the soil during this event (Figure 4.7). This decoupling phenomenon was caused by the soil desiccation and the formation of cracks that occurred around the body of the tensiometers tubes.

www.manaraa.com
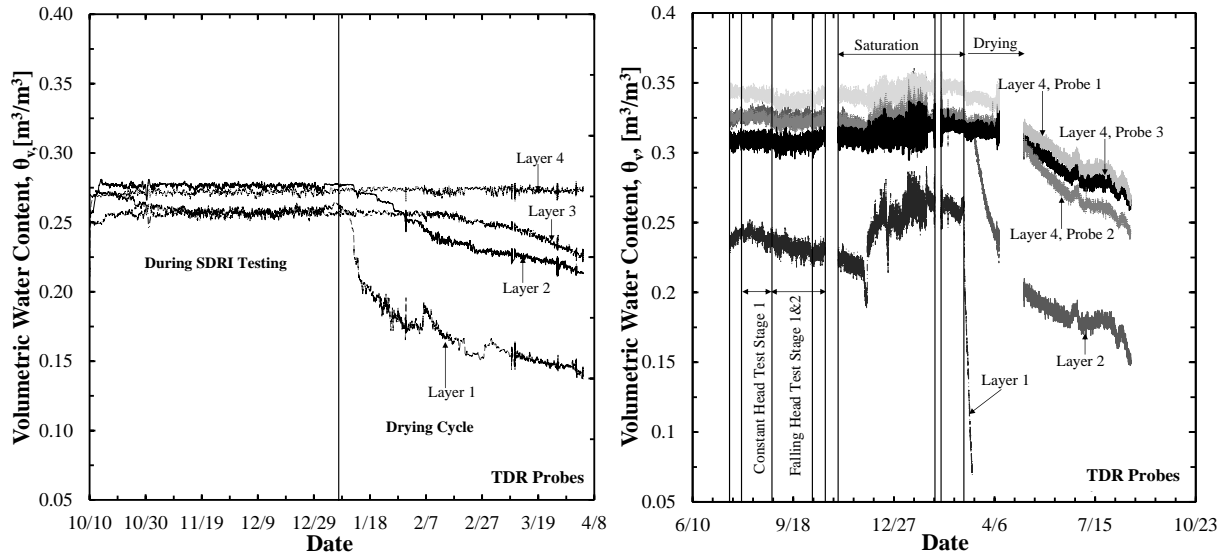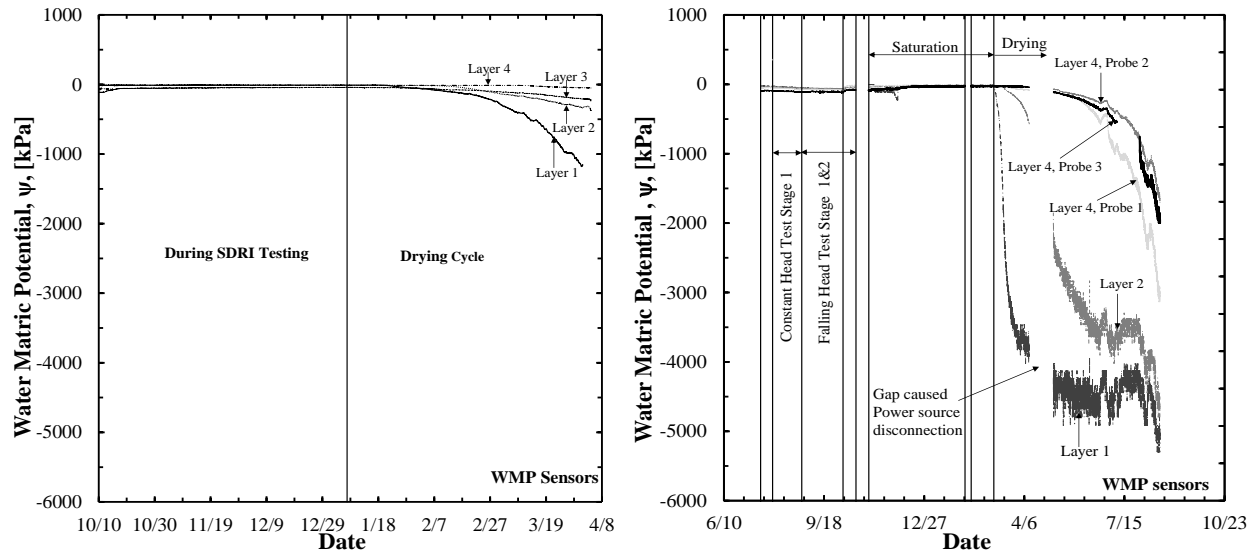
Figure 4.6. Time-dependent response of the TDR probes and the WMP sensors that were located within Test Pad 1 (a,c) and Test Pad 2 (b,d).

64
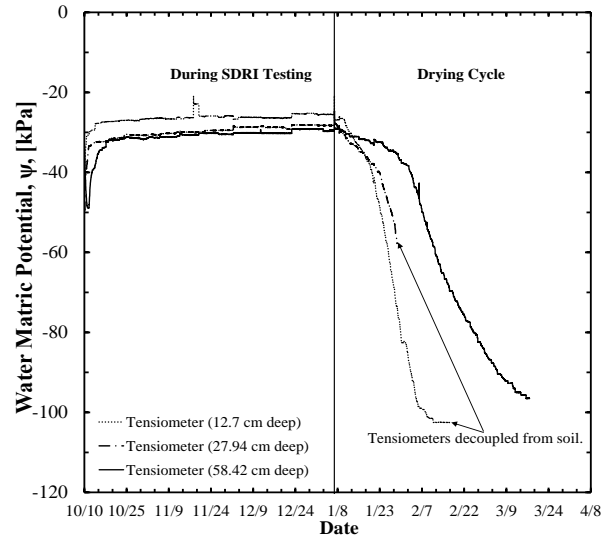
Figure 4.7. Time-dependent response of the tensiometer probes that were installed within Test Pad 1.

4.8.3. Soil Water Characteristic Curve and Hydraulic Conductivity Functions

Based on the volumetric water content and water matric potential measurements that were collected from the in-situ sensors, the field-based SWCCs, at each layer, were determined and are shown in Figure 4.8 for Test Pads 1 and 2. As anticipated, the soil near the surface (Layer 1) dried faster because the top surface of this layer was exposed to the atmospheric conditions; the influence of evaporation decreased as a function of depth from Layer 1 to Layer 4. Based on the data collected from Test Pad 1, the drying cycle was terminated before the drying front reached the probes located within the bottom layer (Layer 4). Therefore, the field-obtained SWCC was not well defined for Layer 4.

65
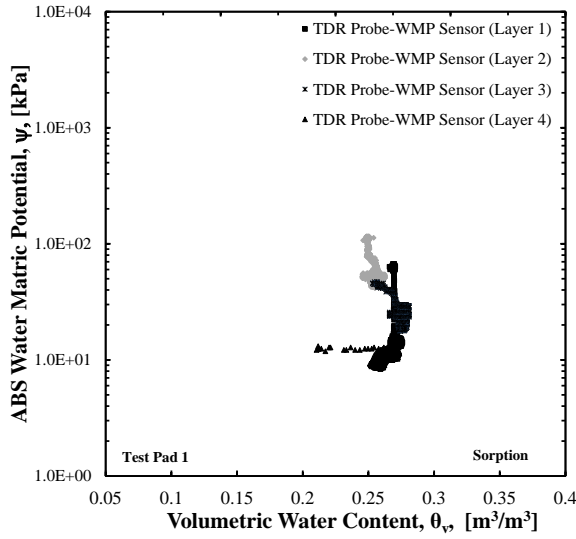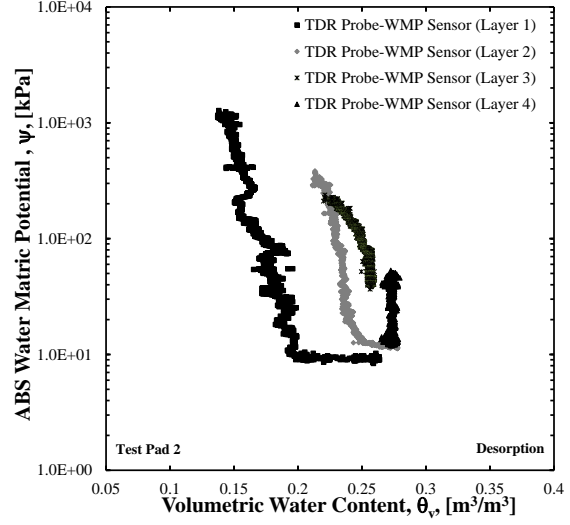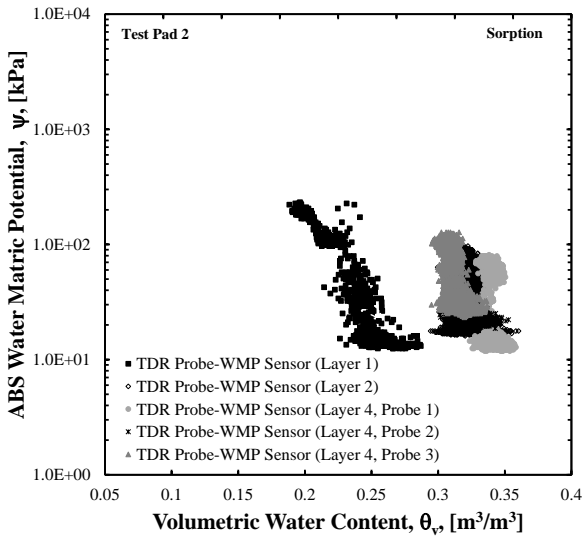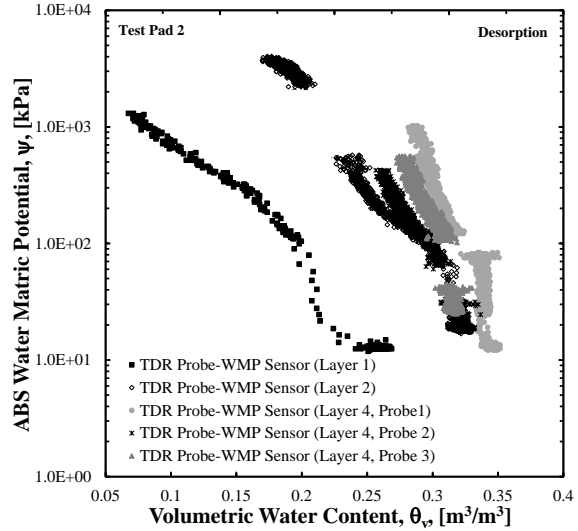
Figure 4.8. Measured volumetric water content and matric potential from Test Pad 1 (a,b) and Test Pad 2 (c,d) using TDR probe data and WMP sensor data during a) the wetting cycle (sorption) and b) the drying cycle (desorption).

As previously noted, the field-obtained wetting curves were not clearly defined for all of the layers. This lack of definition was attributed to: 1) the soil being placed under conditions of high soil-moisture content and 2) the inability of the in-situ instrumentation to accurately measure the small changes in the volumetric water content and the water matric potential within

66

the soil during the saturation phase (Figures 4.8a and 4.8c for Test Pad 1 and 2, respectively).

Layer 1, within Test Pad 2, was placed with a lower average water content (gravimetric and

volumetric) value than the other layers. Therefore, a more well-defined wetting curve was

obtained from Layer 1 of Test Pad 2 than from any other layer. Furthermore, a more clearly

defined desaturation curve was observed for Layer 1, within both Test Pad 1 and Test Pad 2, due

to the previously discussed influence of evaporation on each soil layer (Figures 4.8b and 4.8d,

respectively). Because of the higher quality data obtained from Layer 1 of Test Pad 2 (Figure

4.9), these SWCCs were considered as the representative field-obtained SWCCs for both test

pads. Therefore, these data were utilized for analysis within the RETC computer program, and

were also utilized for comparison with the laboratory-obtained SWCCs and k-functions that were

generated by using the Shelby tube samples that were taken from Layer 2 within Test Pad 1.

Figure 4.9. Field-obtained soil water characteristic curves (from Test Pad 2 Layer 1) that were selected for the RETC analysis.

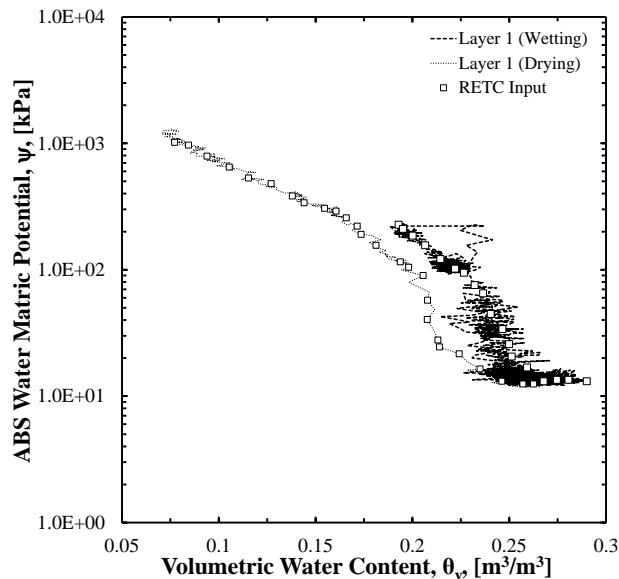The field-obtained SWCCs, presented in Figure 4.9, represented thousands of data points.

However, due to the capacity and limitations within the RETC program to process large data

sets, points were randomly selected ("selected points") from the continuous data, based upon

67

perceived trends within the data. These selected points were then utilized, as input, within the

RETC program to determine the mathematical model for both the SWCC and the k-function. By

comparing the wetting and drying curves, as obtained within Test Pad 2 Layer 1 (Figure 4.9), a

significant hysteresis was observed between the wetting and drying curves. As observed by

previous researches, this hysteresis was attributed to the ink-bottle effect, swelling-shrinking

potential of the clay, and the effects associated with the probes (including measurement error).

As a result of the hysteresis, at a given volumetric water content value, two different values for

water matric potential were obtained (depending on if the soil is undergoing a drying or wetting

cycle).

The van Genuchten hydrological parameters (α, m, n and k_s) that were obtained from

TRIM testing for wetting and drying cycles are summarized in Table 2. The fitting parameters

that were obtained from the RETC program, by inputting the measured volumetric water content

and matric suction values obtained from in-situ sensors and from the WP4 device, are also

presented in Table 3. The well-fitted drying and wetting SWCC and k-function curves, and the

measured data that were obtained from the in-situ sensors (TDR and WMP), TRIM device, and

WP4 are presented in Figure 4.10a.

Table 4.2. van Genuchten fitting parameters of SWCC obtained from TRIM testing.

	θ_r (%)	θ_s (%)	α (1/cm)	n	m	I	k_s (cm/sec)
Wetting Cycle	10	35	0.005	1.21	0.174	0.5	2.6E-07
Drying Cycle	10	39	0.005	1.24	0.190	0.5	5.0E-06

Table 4.3. van Genuchten fitting parameters of SWCC estimated using RETC program.

	Drying Cycle					Wetting Cycle				
	θ_r (%)	θ_s (%)	α (1/cm)	n	m	θ_r (%)	θ_s (%)	α (1/cm)	n	m
TDR & WMP sensors	6.7	31.7	0.012	1.005	0.190	4.8	29.9	0.014	1.005	0.208
WP4	3.7	32.5	0.035	3.828	0.591	10.6	28.5	0.010	3.372	0.066

68
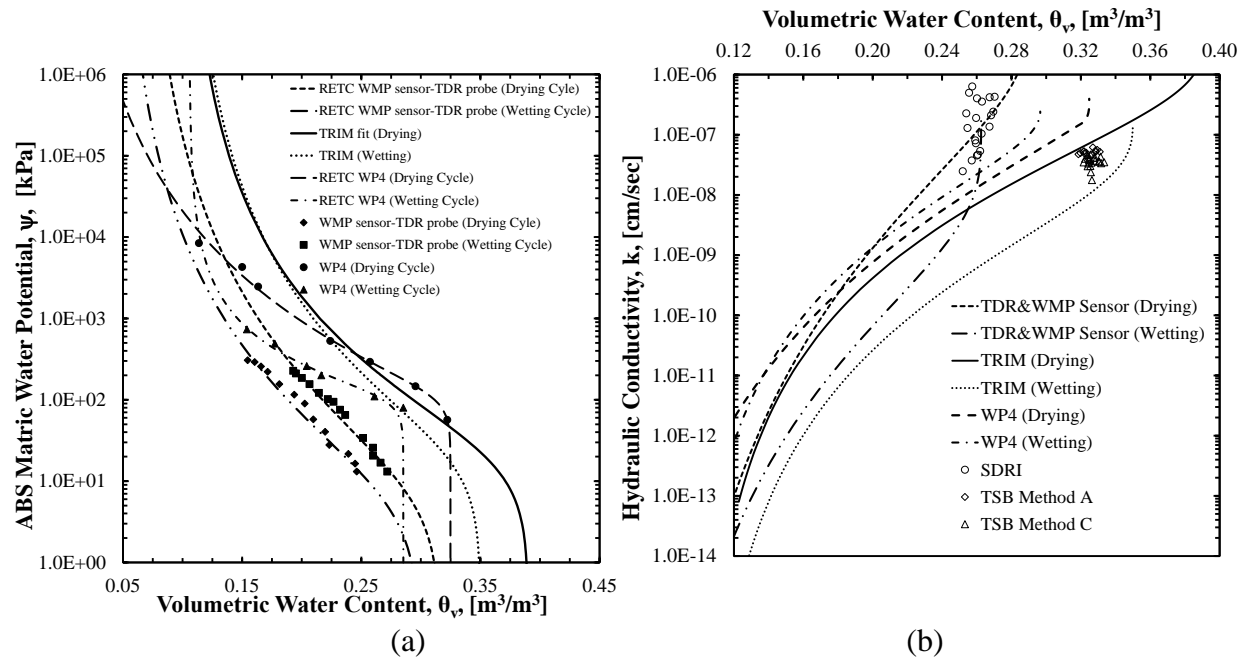
Figure 4.10. Results obtained by using TRIM, WP4, and field-obtained infiltration methods. (a) SWCCs, (b) k-functions along with SDRI, FWP, and TSB data.

As shown in Figure 4.10, the laboratory-obtained drying and wetting curves intersected at the matric suction and volumetric water content values of 1.19×10^4 kPa, and 0.113 for WP4 and at values of 7.30×10^3 kPa and 0.172 for TRIM, respectively. The shapes of the curves that were obtained using these two methods were also different. The wetting and drying curves that were modeled using the data collected from the in-situ sensors data never intersected, but the shape of the field-based SWCCs are similar to the shapes of the laboratory-obtained TRIM curves. In addition, the shapes of the curves obtained from WP4 were different (much flatter) than the other SWCCs that are presented in Figure 4.10a.

The k-functions for the field-obtained data, as predicted based from the measured SWCC and the van Genuchten-Mualem relative hydraulic conductivity model, are shown in Figure 4.10b. The predicted k-functions matched well with the measured k-function obtained during SDRI, as shown in Figure 4.10b; thus proving to be a reasonable validation of the field-obtained

69

method that was used to obtain the SWCC and k-function data. The discrepancy between the measured TSB hydraulic conductivity and the predicted k-functions was attributed to the recorded differences between the saturated volumetric water content (θ_s) values within the testing layers of Test Pad 2. Layer 1, within Test Pad 2, and Layers 1 through 4, within Test Pad 1 had measured $\th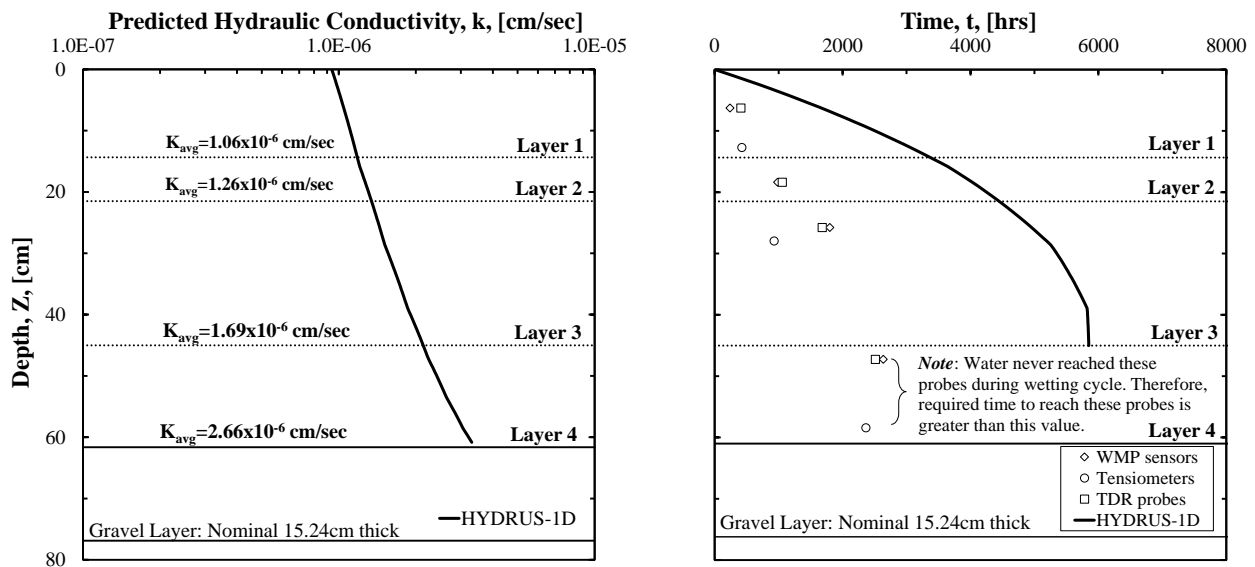eta_s$ values below 30 percent; however, Layers 2 through 4, within Test Pad 2, had a measured θ_s values above 30 percent (as previously presented in Figures 4.6a and 4.6b). As reported in Chiu and Shackelford (1998), variations in the measured and theoretical values for θ_s caused significant differences in the predicted values of hydraulic conductivity. Therefore, differences in measured values for θ_s between layers, like those observed in Test Pad 2, may also have affected the predicted values of hydraulic conductivity.

From Figure 4.10b, the curves fitted by the RETC program using WP4 data have generally the same slope as the curves obtained from the TRIM device. The hydraulic conductivity values that were measured using TRIM and WP4 were lower than the measured field-obtained results from the SDRI and TSB testing. This was attributed to the soil disturbances that were introduced to the TRIM and WP4 samples during the soil sampling preparation process that may have led to: 1) changes in the stress conditions, 2) a reduction of porosity, and 3) an increased amount of sample compaction. Moreover, the difference in particle distribution, which is a function of density, may have also had a significant effect on the water matric potential and the hydraulic conductivity measurements because of the void ratio changed within the soil. Consequently, the array of water matric potential values that were determined by using the WP4 device were not an accurate indicator of the true state of the soil that was used within the clay liner.

70

4.8.4. Measured and Predicted Hydraulic Conductivity and Flow

The predicted hydraulic conductivity as function of depth for Test Pad 1 and 2 are shown in Figure 4.11a and 4.11c, respectively. The HYDRUS-1D predicted higher values than the values that were measured during the field-scale tests. A comparison between the predicted and measured amount of time required for water to flow through each layer, using HYDRUS-1D program and in-situ instrumentation, within Test Pads 1 and 2 are also shown in Figures 4.11a and 4.11b and Figures 4.11c and 4.11d, respectively. Quantifying and predicting the hydrologic responses using HYDRUS-1D model were challenging because the program requires an extensive input of geotechnical parameters such as: saturated-unsaturated hydraulic properties, physical design, root uptake, meteorological conditions and vegetation data that were not available for this analysis. Only saturated in-situ hydraulic conductivity values and fitting parameters (α, m, n) obtained from the measured SWCC were available to be as used as input within the program, and the other parameters were ignored. Therefore, not accounting for all the aforementioned parameters may have led to the predicted hydraulic conductivity values being too low using HYDRUS-1D.
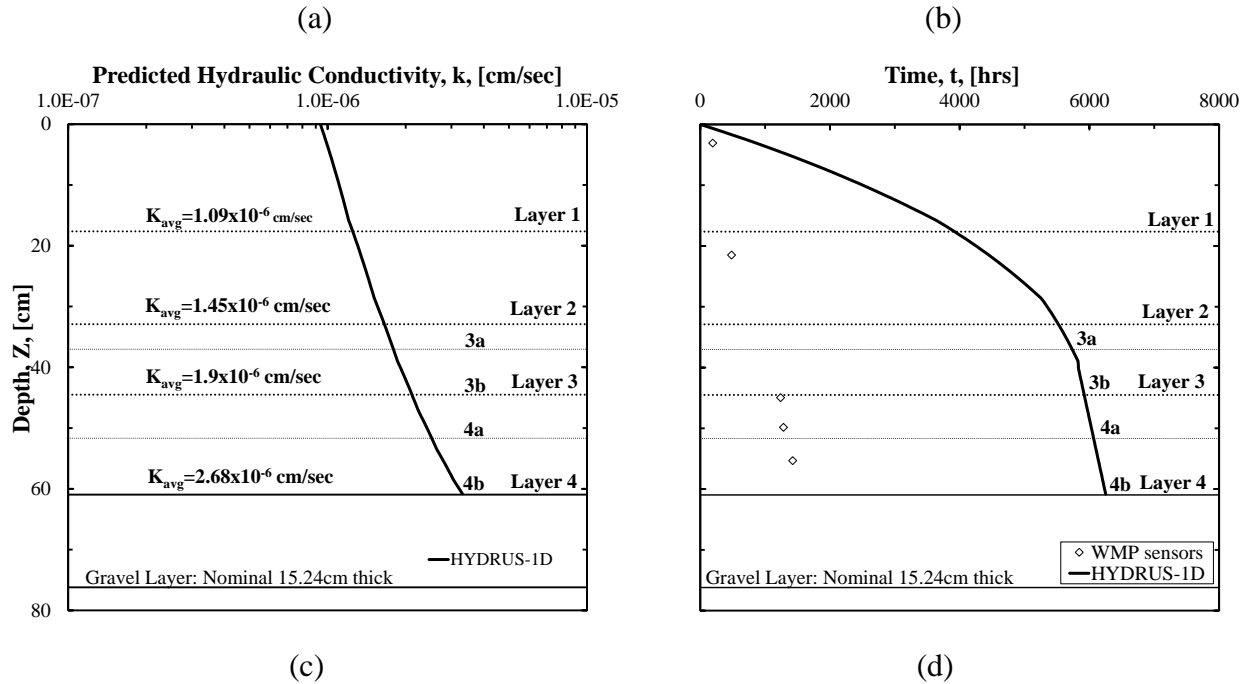
Predicted Hydraulic Conductivity, k, [cm/sec]

1.0E-07   1.0E-06   1.0E-05

Time, t, [hrs]

0   2000   4000   6000   8000

$K_{avg}=1.09\times10^{-6}$ cm/sec   Layer 1

$K_{avg}=1.45\times10^{-6}$ cm/sec   Layer 2

3a

$K_{avg}=1.9\times10^{-6}$ cm/sec   3b   Layer 3

4a

$K_{avg}=2.68\times10^{-6}$ cm/sec   4b   Layer 4

Depth, Z, [cm]

HYDRUS-1D

Gravel Layer: Nominal 15.24cm thick

Layer 1

Layer 2

3a

3b   Layer 3

4a

4b   Layer 4

◇ WMP sensors
— HYDRUS-1D

Gravel Layer: Nominal 15.24cm thick

(c)   (d)

Figure 4.11. (a,c) Predicted hydraulic conductivity values as function of depth obtained using HYDRUS-1D, and (b,d) measured and predicted amount of time required for the wetting front to reach the probes for Test Pad 1 (a,b) and Test Pad 2 (c,d).

The measured hydraulic conductivity values from SDRI were lower than the regulator values (less than 1×10^{-7}cm/sec) in Layer 1 and 2 at the depth of 76.2cm and 59.74cm, respectively, when using the wetting front and suction methods. However, as displayed previously in Figure 4.3a, higher hydraulic conductivity measurements were observed using the apparent method, where the wetting front and suction front were not monitored. Conversely, the values obtained from the TSB testing were also below the regulatory limit. The values predicted using the RETC and HYDRUS-1D computer programs exceeded the regulatory limit at each layer (greater than 1×10^{-7}cm/s). As reported in Chiu and Shackelford (1998), the over-prediction within the RETC program may be caused by inability of capillary tube models (van Genuchten-Mualem for this case) to capture the complexities of unsaturated flow through compacted soils.

72

4.8.5. Effects of Testing Procedures

As previously discussed, the testing procedures that were utilized to collect the field data may have affected the obtained results. The soils that were utilized were placed in accordance to the previously established placement method (as shown previously in Figure 4.5). This placement method and the corresponding zone of acceptance was developed to ensure low values of permeability (wet side of optimum water content) and was not developed to enable the measurement of the sorption SWCC. Layer 1, within Test Pad 2, was placed at a lower value of water content. This lower water content value was observed to improve the measurement of the sorption SWCC relative to the other wetter layers during the infiltration phase. Therefore, to obtain well-defined sorption and desorption curves, a new ZOA should be considered for future test pad investigations that focus on SWCCs.

4.9. Conclusion

A field-method, to attain the SWCC and k-function for a compacted clay liner, was developed by using the data obtained from in-situ instrumentation. Like with any other field instrumentation test, a verification and validation of the "field-obtained" method was performed. The presented results agree with the results of previous studies; there was a poor correlation between field-obtained and laboratory-obtained k-functions. Based upon the obtained results, the following conclusions and recommendation were drawn:

- The shapes of the field and laboratory-obtained SWCC were similar, albeit, at different volumetric water contents.
- Due to the lack of sensitivity of the TDR probes within the wet region, it is recommended that the soil be compacted dry of the utilized ZOA for future laboratory investigations to overcome the difficulty of: 1) capturing the change of volumetric

73

water content during SDRI or TSB testing, and 2) predicting the location of the wetting front during wetting cycle.

- It was determined that changes in θ_s, from a change in soil conditions or saturation, has a substantial impact on the predicted k-function. Therefore, when using the RETC program to determine the SWCC and k-function of a soil, the initial conditions of the soil should be representative of the in-situ soil.

- Because laboratory tests (WP4, TRIM) change the state of the soil, the SWCCs and k-functions determined using these methods may not be characteristic of the in-situ soil. Therefore, it is recommended that only methods that can match the soil state in the field (specifically bulk density, porosity, and water content) be used to determine SWCCs and k-functions.

4.10. References

ASTM (2010). "Standard test method for measurement of hydraulic conductivity of saturated porous materials using a flexible wall permeameter." *ASTM D5084-10*, West Conshohocken, PA.

ASTM (2008). "Standard test methods for field measurement of infiltration using double-ring infiltrometer with sealed-inner ring." *ASTM D5093-02*, West Conshohocken, PA.

ASTM (2006). "Standard test method for field measurement of hydraulic conductivity using borehole infiltration." *ASTM D6391-06*, West Conshohocken, PA.

ASTM (2008). "Standard test methods for determination of the soil water characteristic curve for desorption using a hanging column, pressure extractor, chilled mirror hygrometer, and/or centrifuge." *ASTM D6836-02*, West Conshohocken, PA.

Blanchard, J. (2015). "Evaluation of the equations used to calculate hydraulic conductivity values from two-stage borehole tests." Undergraduate Honors Thesis, University of Arkansas.

Chiu, T.F., and Shackelford, C. (1998). "Unsaturated hydraulic conductivity of compacted sand kaolin mixtures." *J. Geotech. Geoenviron. Eng.,* 10.1061/(ASCE)1090 0241(1998) 124:2(160), 160-170.

Daniel, D. and Benson, C. (1990). "Water content-density criteria for compacted soil liners." *J. Geotech. Engrg.*, 10.1061/(ASCE)0733-9410(1990)116:12(1811), 1811-1830.

Daniel, D., and Trautwein, S. (1986). "Field permeability test for earthen liners." *Proceedings of In Situ '86*, Blacksburg, Va., pp. 146-160.

Fredlund, D. G., Xing, A., and Huang, S. (1994). "Predicting the permeability function for unsaturated soils using the soil-water characteristic curve." *Canadian Geotechnical Journal*, Ottawa, Canada, Vol. 31, No. 4, 1994, 533-546.

Fredlund, D.G. (1995). "Prediction of unsaturated soil functions using the soil-water characteristic curve." unsaturated soils group department of civil engineering. University of Saskatchewan, 57 Campus Drive, Canada, 1995.

Fredlund, D. G. and Rahardjo, H. (1996). Soil mechanics for unsaturated soils, *John Wiley and Sons Inc.*, New York.

Fredlund, M. D., Sillers, W. S., Fredlund, D. G. and Wilson, G. W. (1996). "Design of a knowledge-based system for unsaturated soil properties." *Proceedings of the Canadian Conference on Computing in Civil Engineering,* Montreal, Quebec, August 26-28, pp. 659-677.

Fredlund, D. and Xing, A. 1997. "Equations for the soil water characteristic curve." *Canadian Geotechnical Journal*, Vol. 3, No. 4, 533-546.

Fernando, A. M. (2005). "Nature of soil-water characteristic curve of plastic soils." *J. Geotech. Geoenviron. Eng.*, 10.1061(ASCE) 1090-0241(2005)131:5(654), 654-661.

Johari, A and Nejad, A. H. (2015). "Prediction of soil-water characteristic curve using gene expression programming." IJST, Transactions of Civil Engineering, Vol. 39, No. CI, pp 143-165. Klute, A. Campbell, G.S. Jackson, D. Mortiland, M.M. and Nielson, D.R. (1986). "Methods of soil analysis." Part 1, *Physical and Mineralogical Methods, Second Edition,* American Society of Agronomy and Soil Science of America, Madison, Wisconsin, 810 pgs.

Li, A. G., Tham, L. G., Yue Z. Q., Lee, C. L., and Law K. T. (2004). "Comparison of field and laboratory soil-water characteristic curves." *J. Geotech. Geoenviron. Eng.*, 10.1061/ (ASCE) 1090-0241(2005)131:9(1176), 1176-1180.

Lin, B. and Cerato, A.B. (2012). "Hysteretic water retention behavior of two highly clayey expansive soils." *ASCE Geotechnical Special Publication No. 225, Proc. GeoCongress 2012: State of the Art and Practice in Geotechnical Engineering*, Oakland, California, 1205-1212.

Lu, N. and Likos, W.J. (2004). Unsaturated soil mechanics, *John Wiley and Sons*, New Jersey, USA, 556 pgs.

Lu, N., and Kaya, M. (2013). "A drying cake method for measuring suction stress characteristic curve, soil-water retention, and hydraulic conductivity function." *Geotechnical Testing Journal,* Vol. 36, pp. 1–19.

Lu N., Kaya M., and Godt. W. J. (2014). "Interrelations among the soil-water retention, hydraulic conductivity, and suction-stress characteristic curves." *J. Geotech. Geoenviron. Eng.*, 10.1061/(ASCE)GT.1943-5606.0001085, 04014007.

Maldonado, C., and Coffman, R. (2012). "Hydraulic conductivity of environmentally controlled landfill liner test pad." *ASCE Geotechnical Special Publication No. 225, Proc. GeoCongress 2012: State of the Art and Practice in Geotechnical Engineering*, Oakland, California, 3593-3602.

Meerdink, J. S., Benson, C. H., and Khire, M. V. (1996). "Unsaturated hydraulic conductivity of two compacted barrier soils." *J. Geotech. Engrg.*, 10.1061/(ASCE)0733-9410(1996) 122:7(565), 565-576.

Mijares, R.G. and Khire, M.V. (2010). "Soil water characteristic curves of compacted clay subjected to multiple wetting and drying cycles." *GeoFlorida 2010: Advances in Analysis, Modeling and Design,* ASCE, 400-409.

Mualem, Y. (1976). "A new model for predicting the hydraulic conductivity of unsaturated porous media." *Water Resour. Res.*, Vol. 12, pp. 513-522.

Nanak, M. J. (2012). "Variability in the hydraulic conductivity of a test pad liner system using different testing techniques." *Master's Thesis*, University of Arkansas.

Ogorzalek A. S., Bohnholf G.L., Shackelford C. D., Benson, C. H., and Apiwantragoon. (2008). "Compaction of field data and water-balance predictions for a capillary barrier covers." *J. Geotech. Geoenviron. Eng.*, 10.1061/(ASCE)1090-0241(2008)134:4(470), 470-486.

Simunek, J., Sejna, M., and van Genuchten, M. Th. (1999). "The hydrus-2d software package for simulating the two-dimensional movement of water, heat, and multiple solutes in variably saturated media." IGWMC-TPS 53, version 2, Int. Ground Water Modeling Center, Colorado School of Mines, Golden, Colo.

Soil Testing Engineers, Inc. (1983). "STEI two-stage field permeability test.*"* Soil Testing Engineers, Inc., Baton Rouge, LA.

Trautwein, S. and Boutwell, G. (1994). "In situ hydraulic conductivity tests for compacted soil liners and caps." *Hydraulic Conductivity and Waste Contaminant Transport in Soil, STP 1142, D. Daniel and S. Trautwein, eds.*, ASTM, Philadelphia, 184-223.

Tzimas, E. (1979). "The measurement of soil water hysteretic relationship on a soil monolith." *J. Soil Sci.,* Vol. 30, 529-534.

van Genuchten, M. T. (1991). "The retc code for quantifying the hydraulic functions of unsaturated soils." *U.S. Salinity Laboratory*, Riverside, California.

Wang, X. and Benson, C. (2004). "Leak-free Pressure Plate Extractor for Measuring the Soil Water Characteristic Curve." *Geotechnical Testing Journal*, Vol. 27, No. 2, pp.1-10.

Watson, K.K., Reginato, R. J., and Jackson, R. D. (1975). "Soil water hysteresis in a field soil." *Soil Sci. Soc. Am. Proc.,* Vol. 39, 242-246.

Wayllace, A., and Lu, N. (2012). "A transient water release and imbibitions method for rapidly measuring wetting and drying soil water retention and hydraulic conductivity functions." *Geotechnical Testing Journal*, Vol. 35, No. 1, 1

CHAPTER 5: CONCLUSIONS

5.1. Chapter Overview

The conclusions that were amassed in this work are contained in this chapter. In Section 5.2, a summary of major findings is provided. Limitations of the work that was described in this document are outlined in Section 5.3. Finally, recommendations for future work are provided in Section 5.4.

5.2. Summary

The two-stage borehole (TSB) methods (Method A, Method B, and Method C), as presented in ASTM D6391 (2011) were assessed by 1) examining the evolution of each of the methods in literature and 2) by comparing the results obtained by using each method to evaluate field-scale laboratory compacted clay liners (CCLs). The evaluation of the TSB methods was described in Chapter 3 of this document. Additionally, in-situ instrumentation was utilized within constructed test pads at the University of Arkansas to investigate the observed differences between field-obtained and laboratory-obtained soil water characteristic curves (SWCCs) and hydraulic conductivity functions (k-functions). The observed SWCCs and k-functions were presented in Chapter 4 of this document.

Several errors were observed within the ASTM D6391 (2011) standard. Specifically, errors were observed in: the example data sheets, equations for Method B, and Method C equation. The ASTM data sheets contain numerous errors and should be corrected to avoid causing confusing among practitioners. The equation for Method C was incorrectly derived; the corrected equation and the derivation for the corrected equation were presented in Section 3.7.2. Method B was determined to be under constrained. Two recommendations to improve Method B were provided; 1) a greater number of readings per filling of the standpipe should be acquired

77

and 2) the value of Z* should be independently determined to correspond to the piezometric line. It was recommended that Method B not be utilized until additional guidelines are developed.

The shape of the field-obtained and laboratory-obtained SWCCs were similar; however, the curves corresponded with different values of volumetric water content. The aforementioned difference significantly affected the k-functions. Therefore, when field-obtained SWCCs can be determined, it is recommended that the field-obtained curves be utilized, because the laboratory curves were non-representative. This was attributed to 1) the differing values of saturated volumetric water content that caused the curves to shift along the x-axis, and 2) changes in the soil state during laboratory testing (specifically changes in bulk density, porosity, soil structure, confining stress) that occurred as a result of the soil being disturbed. It was recommended that only laboratory methods that match the field state be utilized to determine SWCCs and k-functions.

5.3. Limitations

Most of the limitations associated with the work presented within this document are in regard to the need for further validation and the incorporation of additional testing methods. Specifically, for the evaluation of TSB methods, the following limitations were observed:

- Although ASTM D6391 (2011) Method B is derived from the velocity method (Chapuis 1999), there are deviations between two methods. Therefore, the velocity method should be further investigated;

- ASTM D6391 (2011) Method C was shown to be less variable, but is only utilized as a Stage 1 test and the value of the vertical hydraulic conductivity was obtained;

- ASTM D6391 (2011) Method B is also only for a one stage test.

For the SWCC and k-functions investigation the following limitation were observed:

78

- Only two laboratory methods were utilized in the comparison; for completeness, results from other common laboratory testing methods should also be compared with the field results;

- It is difficult to determine SWCCs from test pads placed in wet conditions or that only experience small variations in water content;

- Although it is sometimes difficult or impractical to determine SWCCs in the field, additional guidance was provided that may enhance laboratory-obtained SWCCs.

5.4. Recommendations

In accordance with the limitations identified in Section 5.3, the following recommendations are made for future research:

- Additional TSB testing should be performed, with an emphasis on ASTM D6391 (2011) Method B and ASTM D6391 (2011) Method C, under Stage 2 conditions;

- The differences between ASTM D6391 (2011) Method B and other proposed velocity methods (Chapuis 1999, Chiasson 2005) should be further investigated;

- Validation of the observed differences between laboratory and field-obtained SWCCs should be performed, utilizing other common testing methods to determine the SWCC in the laboratory;

- Procedures/guidelines should be developed to enhance laboratory-obtained SWCCs when field-obtained SWCCs are unavailable.

5.5. References

ASTM (2011), "Standard test method for field measurement of hydraulic conductivity using borehole infiltration." Annual Book of ASTM Standards, Designation D 6391-11, Vol. 4.08, ASTM, West Conshohocken, PA.

Chapuis, R., (1999). "Borehole variable-head permeability tests in compacted clay liners and covers." *Canadian Geotechnical Journal*, Vol. 36, pp. 39-51.

Chiasson, P., (2005). "Methods of interpretation of borehole falling-head tests performed in compacted clay liners." *Canadian Geotechnical Journal*, Vol. 42, pp. 79-90.

CHAPTER 6: REFERENCES

ASTM (2016). "Standard test method for measurement of hydraulic conductivity of saturated porous materials using a flexible wall permeameter." *ASTM D5084-10*, West Conshohocken, PA.

ASTM (2015). "Standard test methods for field measurement of infiltration using double-ring infiltrometer with sealed-inner ring." *ASTM D5093-15*, West Conshohocken, PA.

ASTM (2011), "Standard test method for field measurement of hydraulic conductivity using borehole infiltration." Annual Book of ASTM Standards, Designation D 6391-11, Vol. 4.08, ASTM, West Conshohocken, PA.

ASTM (2006), "Standard test method for field measurement of hydraulic conductivity using borehole infiltration." *ASTM D6391-06*, West Conshohocken, PA.

ASTM (1999), "Standard test method for field measurement of hydraulic conductivity limits of porous materials using two stages of infiltration from a borehole" Annual Book of ASTM Standards, Designation D 6391-99, Vol. 4.08, ASTM, West Conshohocken, PA.

ASTM (2016), "Standard test methods for determination of the soil water characteristic curve for desorption using a hanging column, pressure extractor, chilled mirror hygrometer, and/or centrifuge." *ASTM D6836-16*, West Conshohocken, PA.

ASTM (2017), "Standard test method for in-place density and water content of soil and soil-aggregate by nuclear methods (shallow depth)." Annual Book of ASTM Standards, Designation D 6938, Vol. 4.08, ASTM, West Conshohocken, PA.

Blanchard, J. (2015). "Evaluation of the equations used to calculate hydraulic conductivity values from two-stage borehole tests." Undergraduate Honors Thesis, University of Arkansas.

Boutwell, G., (1992). "The STEI two-stage borehole field permeability test." Containment Liner Technology and Subtitle D, Houston Section, ASCE, Houston, TX.

Boutwell, G. and Tsai, C., (1992). "The two-stage field permeability test for clay liners." *Geotechnical News*, C. Shackelford and D. Daniel, eds., pp. 32-34.

Chapuis, R., (1999). "Borehole variable-head permeability tests in compacted clay liners and covers." *Canadian Geotechnical Journal*, Vol. 36, pp. 39-51.

Chiasson, P., (2005). "Methods of interpretation of borehole falling-head tests performed in compacted clay liners." *Canadian Geotechnical Journal*, Vol. 42, pp. 79-90.

Chiu, T.F., and Shackelford, C. (1998). "Unsaturated hydraulic conductivity of compacted sand kaolin mixtures." *J. Geotech. Geoenviron. Eng.,* 10.1061/(ASCE)1090 0241(1998) 124:2(160), 160-170.

Daniel, D., (1989). "In situ hydraulic conductivity tests for compacted clay." *Journal of Geotechnical Engineering*., ASCE, Vol. 115, No. 9, pp. 1205-1226.

Daniel, D. and Benson, C. (1990). "Water content-density criteria for compacted soil liners." *J. Geotech. Engrg.*, 10.1061/(ASCE)0733-9410(1990)116:12(1811), 1811-1830.

Daniel, D., and Trautwein, S. (1986). "Field permeability test for earthen liners." *Proceedings of In Situ '86*, Blacksburg, Va., pp. 146-160.

Fredlund, D. G., Xing, A., and Huang, S. (1994). "Predicting the permeability function for unsaturated soils using the soil-water characteristic curve." *Canadian Geotechnical Journal*, Ottawa, Canada, Vol. 31, No. 4, 1994, 533-546.

Fredlund, D.G. (1995). "Prediction of unsaturated soil functions using the soil-water characteristic curve." unsaturated soils group department of civil engineering. University of Saskatchewan, 57 Campus Drive, Canada, 1995.

Fredlund, D. G. and Rahardjo, H. (1996). Soil mechanics for unsaturated soils, *John Wiley and Sons Inc.*, New York.

Fredlund, M. D., Sillers, W. S., Fredlund, D. G. and Wilson, G. W. (1996). "Design of a knowledge-based system for unsaturated soil properties." *Proceedings of the Canadian Conference on Computing in Civil Engineering,* Montreal, Quebec, August 26-28, pp. 659-677.

Fredlund, D. and Xing, A. 1997. "Equations for the soil water characteristic curve." *Canadian Geotechnical Journal*, Vol. 3, No. 4, 533-546.

Fernando, A. M. (2005). "Nature of soil-water characteristic curve of plastic soils." *J. Geotech. Geoenviron. Eng.*, 10.1061(ASCE) 1090-0241(2005)131:5(654), 654-661.

Garner, C. (2017). "Development of a multiband remote sensing system for determination of unsaturated soil properties." Doctoral Dissertation, University of Arkansas.

Gee, G., M. Campbell, G. Campbell, and J. Campbell. 1992. Rapid measurement of low soil potentials using a water activity meter. Soil Sci. Soc. Am. J. 56:1068–1070

Hvorslev, J., (1951). "Time lag and soil permeability in ground water observations." Bulletin No. 36, United States Army Corps of Engineers, Waterways Experiment Station, Vicksburg, MS.

Ishimwe, E, (2014). Field-obtained soil water characteristic curves and hydraulic conductivity functions. Masters Thesis, University of Arkansas, May 2013.

Johari, A and Nejad, A. H. (2015). "Prediction of soil-water characteristic curve using gene expression programming." IJST, Transactions of Civil Engineering, Vol. 39, No. CI, pp 143-165.

Klute, A. Campbell, G.S. Jackson, D. Mortiland, M.M. and Nielson, D.R. (1986). "Methods of soil analysis." Part 1, *Physical and Mineralogical Methods, Second Edition,* American Society of Agronomy and Soil Science of America, Madison, Wisconsin, 810 pgs.

Li, A. G., Tham, L. G., Yue Z. Q., Lee, C. L., and Law K. T. (2004). "Comparison of field and laboratory soil-water characteristic curves." *J. Geotech. Geoenviron. Eng.*, 10.1061/ (ASCE) 1090-0241(2005)131:9(1176), 1176-1180.

Lin, B. and Cerato, A.B. (2012). "Hysteretic water retention behavior of two highly clayey expansive soils." *ASCE Geotechnical Special Publication No. 225, Proc. GeoCongress 2012: State of the Art and Practice in Geotechnical Engineering*, Oakland, California, 1205-1212.

Lu, N. and Likos, W.J. (2004). Unsaturated soil mechanics, *John Wiley and Sons*, New Jersey, USA, 556 pgs.

Lu, N., and Kaya, M. (2013). "A drying cake method for measuring suction stress characteristic curve, soil-water retention, and hydraulic conductivity function." *Geotechnical Testing Journal,* Vol. 36, pp. 1–19.

Lu N., Kaya M., and Godt. W. J. (2014). "Interrelations among the soil-water retention, hydraulic conductivity, and suction-stress characteristic curves." *J. Geotech. Geoenviron. Eng.*, 10.1061/(ASCE)GT.1943-5606.0001085, 04014007.

Malaya, C., & Sreedeep, S. (2012). Critical review on the parameters influencing soil-water characteristic curve. Journal of Irrigation and Drainage Engineering, 138(1), 55-62.

Maldonado, C., and Coffman, R. (2012). "Hydraulic conductivity of environmentally controlled landfill liner test pad." *ASCE Geotechnical Special Publication No. 225, Proc. GeoCongress 2012: State of the Art and Practice in Geotechnical Engineering*, Oakland, California, 3593-3602.

Meerdink, J. S., Benson, C. H., and Khire, M. V. (1996). "Unsaturated hydraulic conductivity of two compacted barrier soils." *J. Geotech. Engrg.*, 10.1061/(ASCE)0733-9410(1996) 122:7(565), 565-576.

Mijares, R.G. and Khire, M.V. (2010). "Soil water characteristic curves of compacted clay subjected to multiple wetting and drying cycles." *GeoFlorida 2010: Advances in Analysis*, *Modeling and Design,* ASCE, 400-409.

Mualem, Y. (1976). "A new model for predicting the hydraulic conductivity of unsaturated porous media." *Water Resour. Res.*, Vol. 12, pp. 513-522.

Nanak, M. J. (2012). "Variability in the hydraulic conductivity of a test pad liner system using different testing techniques." *Master's Thesis*, University of Arkansas.

Ogorzalek A. S., Bohnholf G.L., Shackelford C. D., Benson, C. H., and Apiwantragoon. (2008). "Compaction of field data and water-balance predictions for a capillary barrier covers." *J. Geotech. Geoenviron. Eng.*, 10.1061/(ASCE)1090-0241(2008)134:4(470), 470-486.

Samingan, A., & Schanz, T. (2005). "Comparison of four methods for measuring total suction." *Vadose Zone Journal,* 4(4), 1087-1095.

Simunek, J., Sejna, M., and van Genuchten, M. Th. (1999). "The hydrus-2d software package for simulating the two-dimensional movement of water, heat, and multiple solutes in variably saturated media." IGWMC-TPS 53, version 2, Int. Ground Water Modeling Center, Colorado School of Mines, Golden, Colo.

Soil Testing Engineers, Inc. (1983). "STEI two-stage field permeability test." Soil Testing Engineers, Inc., Baton Rouge, LA.

Tinjum, J.M., Benson, C.H., and Boltz, L.R,.(1997). "Soil-water characteristic curves for compacted clays." *Journal of geotechnical and geoenvironmental engineering* 123, no. 11: 1060-1069.

Trautwein, S. and Boutwell, G. (1994). "In situ hydraulic conductivity tests for compacted soil liners and caps." *Hydraulic Conductivity and Waste Contaminant Transport in Soil, STP 1142, D. Daniel and S. Trautwein, eds*., ASTM, Philadelphia, 184-223.

Tzimas, E. (1979). "The measurement of soil water hysteretic relationship on a soil monolith." *J. Soil Sci.,* Vol. 30, 529-534.

van Genuchten, M. T. (1991). "The retc code for quantifying the hydraulic functions of unsaturated soils." *U.S. Salinity Laboratory*, Riverside, California.

Wang, X. and Benson, C. (2004). "Leak-free Pressure Plate Extractor for Measuring the Soil Water Characteristic Curve." *Geotechnical Testing Journal*, Vol. 27, No. 2, pp.1-10.

Watson, K.K., Reginato, R. J., and Jackson, R. D. (1975). "Soil water hysteresis in a field soil." *Soil Sci. Soc. Am. Proc.,* Vol. 39, 242-246.

Wayllace, A., and Lu, N. (2012). "A transient water release and imbibitions method for rapidly measuring wetting and drying soil water retention and hydraulic conductivity functions." *Geotechnical Testing Journal*, Vol. 35, No. 1, 1-15.